# MODEL CODE FOR DESIGN OF FLOATING PLATFORMS:

## Phase II - Calibration
## Final Report

Prepared for

Conoco, Inc.
P.O. Box 2197
Houston, Texas 77252

by

Risk Engineering, Inc.
5255 Pine Ridge Road
Golden, Colorado 80403

March 18, 1993

## CONTENTS

# INTRODUCTION

This report documents the results from the second phase of a study to develop prototype probability-based code design equations for the global limit states of tension leg platforms (TLPs). This first phase consisted of the calculation of cumulative distributions of the main global responses (i.e., maximum offset, maximum tension, minimum tension, and air gap), and the calculation of failure probabilities due to combined tension and bending, for three hypothetical platforms with characteristics similar to those of the Jolliett, Hutton, and Heidrun platforms. These calculations explicitly considered the time-variant nature of TLP behavior during severe storms; separate terms are used to model the major components of TLP time-variant response (i.e., first- and second-order wave-induced, and wind-induced). Results from Phase-I of this study are documented in a separate report (Risk Engineering, 1992).

The second phase of this study consists of the probabilistic calibration of code equations for tendon design and for the checking of maximum offset, minimum tension, and air gap. In order to obtain a large enough population of platforms for this calibration, a number of hypothetical platforms are generated by scaling the size and water depth of the three available design, obtaining a total of 22 platforms. Probability analyses similar to those of phase I are performed for all these platforms and the results are used to calculate load[1] and resistance factors. Multiple formats are investigated in order to obtain a balance between accuracy and simplicity.

The calibration of equations for tendon design is conceptually the simplest and it follows the conventional approach to calibration. The objective is to obtain a set of load and resistance factors such that the tendons designed using the factored loads and capacities have safety indices as close as possible to a target safety index. As part of this tendon "design process", it is assumed that the tendon cross-sectional area may be varied within reasonable limits, without changing the values of the TLP static and dynamic global-response components (i.e., tension forces and offsets)[2].

The calibration of maximum offset, minimum tension, and air gap is somewhat different. One cannot vary a scalar design parameter (e.g., increase deck elevation in order to reduce the probability of wave impact on the deck), without changing the values of one or more of the global-response components. Thus, our approach is to develop load factors such that the global response calculated using those factors has a safety index as close as possible to the target safety

---

[1]More precisely, we calibrate load-effect factors. We will refer to these as load factors for the sake of tradition and in order to be more concise.

[2]This is true for the response quantities considered in phases I and II of this study, but it is not true for the springing and ringing responses (which depend on the tendons' axial stiffness). The effects of these additional responses may be considered in a future study.

index[3]. The results from these calibrations are a set of equations and load factors to calculate the offset, minimum tension, and setdown-plus-crest associated with certain exceedance probabilities. The equations and load factors for air gap can be used for setting the air gap. The equations and load factors for offset and minimum tension can be used for checking against allowable values.

For more severe related limit states (i.e., tendon capacity and air gap), we perform the calibration for safety indices of 3 and 4 (corresponding to failure or exceedance probabilities of $10^{-3}$ and $3\ 10^{-5}$). For less severe limit states (i.e., maximum offset and minimum tension), we perform the calibration for safety indices of 3 and 3.5 (corresponding to failure or exceedance probabilities of $10^{-3}$ and $2x10^{-4}$).

This report begins with a description of the scaling relationships that were employed to calculate the response equations for the 19 hypothetical platforms from those for the three platforms analyzed in phase I. This is followed by the description of the characteristic environment that will be used in the calibration and by documentation of the methods followed and results obtained in the calibration of each limit state. Finally, there is a discussion of the calibration results.

## PLATFORM SCALING

Conoco generated 17 hypothetical platforms from the three platforms considered in the Phase-I report, by means of scaling. The objective was to have population of platforms that is large enough and covers an adequate range of designs, to allow the calibration to take place.

Two types of scaling were used. In the first type of scaling, all linear dimensions of the platform (as well as water depth) are scaled up or down by a constant factor. In the second type of scaling, water depth is varied while all platform dimensions other than tendon length remain constant. Table 1 shows all combinations of platform and scaling considered. Conoco excluded those combinations that were considered implausible

[3]Because we do not define a capacity for these limit states, the term "safety index" does not have its usual meaning. The safety index simply represents $-\Phi^{-1}[p(x)]$ where p(x) is the annual probability that the extreme response exceeds a value x of interest.

**Table 1**
Scaled Platforms Considered

| Scaling | GMS | NSS | NSC |
|---|---|---|---|
| *0.75 | | x | x |
| *0.85 | | x | x |
| *0.95 | | x | x |
| *1.00 | x | x | x |
| *1.05 | x | x | |
| *1.15 | x | x | |
| *1.25 | x | x | |
| 250 m | x | | |
| 500 m | x | x | x |
| 1000 m | x[1] | x | x[1] |

[1] The tendon diameter/thickness ratios for these designs were changed to 20 and 21, respectively, in order to increase the tendons' hydrostatic capacity.

The response equations for the scaled platforms were obtained from the regression equations developed by OSAC (1992) using dimensional analysis[4]. For size scaling, each coefficient is scaled according to its units as follows: units of length scale as $L/L_0$, units of force scale as $(L/L_0)^3$, and units of time scale as $(L/L_0)^{1/2}$ (where L is the modified size and $L_0$ is the base size). For depth scaling, static offsets are multiplied by $L/L_0$, and all coefficients in the equations for low-frequency offsets are multiplied by $(L/L_0)^{1/2}$ (where L is now the modified tendon length and $L_0$ is the base tendon length).

The depth scaling of the offset induced by low-frequency wind ($X_{lfw}$) led to counter-intuitive results. Thus, it was necessary to develop a different, more physical equation for the rms value of $X_{lfw}$ to use for depth scaling. This equation takes the form[5]

$$X_{lfw,rms} = \frac{a_1 V_W^2}{\sqrt{1 + a_3 X_s^2}} \qquad (1)$$

[4]Sources: R. Jefferys, Conoco, telefaxes to A. Kumar dated July 24, 1992, and September 24, 1992; R. Jefferys and A. Kumar, memorandum to Model Code JIP Participants dated July 24, 1992.

[5]Source: R. Jefferys, Conoco, telefax to G. Toro and H. Banon dated January 20, 1993.

where $a_1$ and $a_3$ are constant coefficients, $V_W$ is the wind velocity, and $X_S$ is the static offset. $a_3$ is calculated from the platform geometry and pretension; $a_1$ is calculated by assuming that Equation 1 and OSAC's equation predict the same value of $X_{lfw,rms}$ for $H_S$=13 m. The values of $a_1$ and $a_3$ are tabulated below:

| Platform | $a_1$ ($s^2/m$) | $a_3$ ($m^{-2}$) |
|---|---|---|
| GMS | 2.27E-3 | 9.50E-5 |
| NSS | 1.56E-3 | 4.26E-4 |
| NSC | 3.53E-3 | 1.54E-4 |

For the platforms with scaled water depths, $a_1$ scales as $(L/L_0)^{1/2}$ and $a_3$ scales as $(L/L_0)^{-1}$, where L is the modified tendon length and $L_0$ is the base tendon length).

## CHARACTERISTIC ENVIRONMENT

The selection of characteristic environment for the calibrations in this study was guided by the results from the probabilistic analysis documented in the Phase-I report. Tables 2 and 3 show the values of the environmental variables at the design points associated with annual probabilities of exceedance of 1/100 and 1/1000, for all global responses. These values indicate the values of environmental variables that contribute the most to the probability of exceeding the 100- and 1000-year values of the response. Examination of these tables indicate that the design-point values of the environment are similar across platforms and across responses (with the exception of air gap). For responses other than air gap, the design-point values of $H_S$ for the 100- and 1000-year responses have exceedance probabilities of approximately 0.025 and 0.005, respectively. For air gap, the design-point values of $H_S$ are higher and have exceedance probabilities of approximately 0.01 and 0.001, respectively. Examination of importance factors for the other environment variables (i.e., wave peak period, wave direction, wind velocity, wind direction, current velocity, and current direction; see Phase-I report for importance factors) indicates that these variables take values not too different from their expected values given $H_S$.

Based on the above observations, and for he sake of simplicity, the characteristic environment was selected as consisting of the 100-year value of $H_S$ and the (conditional) expected wind and current velocities given the 100-year $H_S$. In addition, we consider the environment associated with the 1000-year value of $H_S$ in the air-gap calibration (because the design-point $H_S$ is higher for air gap and because of the nonlinear effect of setdown). Also for the sake of simplicity, the wave, wind, and current directions are assumed to be in line. The resulting values of the environment variables are obtained using the Gulf of Mexico environmental model described in the phase-I report and are listed in Table 4. The duration of the strongest phase of the storm is taken as 3 hours.

**Table 2**
Values of Environment Variables at 100-Year Design Point

| Limit State | TLP | Lim.State Value | Safety Index | Hs (m) | Tp (sec) | θ(v) (deg) | Vw (m/sec) | θ(w) (deg) | Vc (m/sec) | θ(c) (deg) |
|---|---|---|---|---|---|---|---|---|---|---|
| Offset | GMS | 43.3 | 2.33 | 10.1 | 13.0 | -76 | 35.8 | -76 | 0.88 | -62 |
| Offset | NSS | 15.8 | 2.33 | 10.5 | 13.2 | -76 | 37.3 | -76 | 0.93 | -62 |
| Offset | NSC | 35.4 | 2.33 | 10.6 | 13.2 | -76 | 37.6 | -76 | 0.94 | -62 |
| Max. Tension | GMS | 5690 | 2.33 | 10.4 | 13.2 | -83 | 36.5 | -80 | 0.90 | -65 |
| Max. Tension | NSS | 12300 | 2.33 | 10.6 | 13.3 | -83 | 37.2 | -82 | 0.92 | -65 |
| Max. Tension | NSC | 18400 | 2.33 | 10.4 | 13.2 | -81 | 36.8 | -81 | 0.91 | -65 |
| Min. Tension | GMS | 1870 | 2.33 | 10.4 | 13.2 | -85 | 35.5 | -83 | 0.86 | -64 |
| Min. Tension | NSS | 4380 | 2.33 | 10.7 | 13.3 | -84 | 37.2 | -83 | 0.92 | -65 |
| Min. Tension | NSC | 8070 | 2.33 | 10.5 | 13.2 | -83 | 36.8 | -84 | 0.90 | -63 |
| Air Gap | GMS | 14.1 | 2.33 | 11.7 | 13.7 | -76 | 40.3 | -76 | 1.03 | -62 |
| Air Gap | NSS | 13.5 | 2.32 | 11.8 | 13.8 | -76 | 40.3 | -76 | 1.03 | -61 |
| Air Gap | NSC | 13.8 | 2.33 | 11.8 | 13.8 | -76 | 40.7 | -76 | 1.04 | -61 |

**Table 3**
Values of Environment Variables at 1000-Year Design Point

| Limit State | TLP | Lim.State Value | Safety Index | Hs (m) | Tp (sec) | θ(v) (deg) | Vw (m/sec) | θ(w) (deg) | Vc (m/sec) | θ(c) (deg) |
|---|---|---|---|---|---|---|---|---|---|---|
| Offset | GMS | 64.8 | 3.09 | 12.2 | 13.9 | -76 | 44.2 | -74 | 1.17 | -65 |
| Offset | NSS | 26.3 | 3.09 | 12.8 | 14.2 | -76 | 47.0 | -75 | 1.26 | -63 |
| Offset | NSC | 57.3 | 3.08 | 12.7 | 14.2 | -76 | 46.8 | -75 | 1.25 | -63 |
| Max. Tension | GMS | 6740 | 3.09 | 12.5 | 14.0 | -84 | 44.9 | -81 | 1.19 | -69 |
| Max. Tension | NSS | 14100 | 3.09 | 13.0 | 14.3 | -85 | 46.6 | -84 | 1.23 | -68 |
| Max. Tension | NSC | 21400 | 3.09 | 12.7 | 14.1 | -84 | 45.8 | -83 | 1.22 | -69 |
| Min. Tension | GMS | 1370 | 3.09 | 12.2 | 13.9 | -87 | 41.5 | -86 | 1.05 | -61 |
| Min. Tension | NSS | 2910 | 3.09 | 13.0 | 14.3 | -86 | 46.1 | -86 | 1.20 | -65 |
| Min. Tension | NSC | 6380 | 3.09 | 12.6 | 14.1 | -85 | 44.8 | -88 | 1.15 | -59 |
| Air Gap | GMS | 19 | 3.09 | 13.9 | 14.6 | -76 | 48.8 | -75 | 1.32 | -64 |
| Air Gap | NSS | 17.6 | 3.09 | 14.1 | 14.7 | -76 | 48.3 | -76 | 1.30 | -62 |
| Air Gap | NSC | 18.5 | 3.09 | 14.1 | 14.7 | -76 | 49.7 | -75 | 1.35 | -64 |

**Table 4**
Characteristic Environments

| Quantity | 100 years | 1000 years |
|---|---|---|
| Significant Wave Height ($H_S$, m) | 11.7 | 14.3 |
| Peak wave period ($t_p$, sec) | 13.8 | 14.9 |
| Wind speed ($V_W$, m/sec) | 39.6 | 48.0 |
| Current speed ($V_C$, m/sec) | 1.00 | 1.27 |
| Astronomical tide (m) | +0.6 | +0.6 |
| Storm surge (m) | +0.35 | +0.43 |

Note: tide and surge are considered only in the air gap calculations.

## CALIBRATION FOR COMBINED AXIAL, BENDING, AND HYDROSTATIC STRESSES

It is useful to begin the presentation by describing the steps that would be followed by an engineer who is designing the tendons for a TLP, using the polynomial equations and interaction equation that were used in the phase-I calculations. These steps are as follows:

1. Calculate the values of the response components (offsets, tensions, zero-crossing periods), assuming that the environment quantities take on their characteristic values. We call these the characteristic values of the response quantities.

2. Apply the corresponding load factor $\gamma$ to the characteristic value of each response component and then combine the factored responses. The total tension is calculated as follows:

$$T_{\max}=T_0+\gamma_{sd}T_{sd}+\gamma_{mom}T_{mom}+\gamma_{dyn}\left[\sum_i (B_i\gamma_i T_i)^2\right]^{1/2} \qquad (2)$$

where all T's on the right-hand side represent characteristic values of the various components of tension, the $\gamma$'s represent load factors and the $B_i$'s represent mean peak factors (calculated as $B_i=[2\ln(n_i)]^{1/2}$ where $n_i$ is the number of cycles of dynamic tension). $T_0$ represents pretension, $T_{sd}$ represents the static tension due to setdown, $T_{mom}$ is the static tension due to (mean wind, wave, and current-induced) moments acting on the hull. The $T_i$'s represent root-mean-square (rms) values of the dynamic components of tension, as follows: (1) first-order wave-frequency tension $T_{1v}$, (2) second-order low-

frequency wave-induced tension (including inertia forces) $T_{2v}$, and (3) wind-induced surge and pitch tensions $T_{w,s\text{-}p}$. The tensile force obtained from Equation 2 is the divided by the tendon area to calculate the axial (tensile) stress.

A similar equation is used to calculate maximum offset, i.e.,

$$X_{max}=\gamma_{Xmax}\left\{\gamma_s X_s+\gamma_{dyn}\left[\sum_i (B_i\gamma_i X_i)^2\right]^{1/2}\right\} \tag{3}$$

where the X's represent characteristic values of the various components of offset and the $\gamma_i$'s and $B_i$'s have the same meaning as for Equation 2 (although their values are, in general, different between the two equations). $X_s$ is the static offset (due to wind, current, and wave-drift forces), and the $X_i$'s represent rms values of dynamic components of offsets, as follows: first-order wave-frequency offset $X_{1v}$, (2) second-order low-frequency wave-induced offset $X_{2v}$, and (3) low-frequency wind-induced offset $X_{lfw}$. The maximum offset is then used to calculate the bending moment near the lower end of the tendon. The load factors inside braces in Equation 3 are, for the sake of simplicity, the same factors obtained from the calibration of maximum offset.

The calculated tensile and bending stresses are then introduced into the checking equation for combined stresses. This equation is of the form[6]:

$$\frac{p}{\phi_c P_c}+\left[\frac{f_a}{\phi_y F_a}+\frac{f_b}{\phi_b F_b}\right]^n \le 1 \tag{4}$$

where p, $f_a$, and $f_b$ represent the hydrostatic pressure, axial stress, and bending stress; $P_c$, $F_a(\bullet)$, and $F_b(\bullet)$ represent the corresponding nominal capacities, the $\phi$'s represent capacity factors, and n is a function of $\frac{f_a}{\phi_y F_a}$ , $\frac{f_b}{\phi_b F_b(\cdot)}$, and the tendon's diameter/ thickness ratio (see Phase-I report). $F_a$ is the nominal axial strength, which is equal to the nominal yield strength $F_y$; $P_c(\bullet)$ and $F_b(\bullet)$ are calculated from the factored axial strength $\phi_y F_a$ [7]. In

---

[6]Source: R. Rashedi, Conoco, written communications to G. R. Toro, May 19, 1992, and July 20, 1992.

[7]The axial and bending capacities are calculated as follows. The axial capacity $P_c(\phi_y F_y)$ is calculated as the smaller solution to the equation

$$(P_C-P_E)(P_c-P_0)=P_C P_E(3\Delta D/\tau)$$

addition to the variability in $F_y$, there is subjective uncertainty in the bending and hydrostatic capacities; hence the resistance factors $\phi_b$ and $\phi_c$ (see Phase-I report for further details).

3. The tendon area (and perhaps its diameter/thickness ratio) is then varied until the above equation is satisfied.

The objective of the calibration is to find the optimal values (or at least acceptable values) of all tension load factors in Equation 2, factor $\gamma_{X_{max}}$ in Equation 3[8], and the capacity factors in Equation 4, so that tendons designed using these factors have safety indices close to a target safety index. Mathematically, this is achieved by minimizing the sum of squared differences between the safety index of the structure (as designed) and the target safety index[9]. We perform this calibration for target safety indices of 3 and 4.

The first step in this calibration is to perform probabilistic analyses for all 22 TLP structures, considering multiple values of the tendon cross-section area (the tendon diameter/thickness ratio is kept constant as the cross-section area is varied). Figures 1 through 3 show the resulting relationships between tendon area and safety index.

The second step in the calibration is to obtain initial values of the load and capacity factors. For each TLP, one finds the tendon area associated with the target safety index (using the corresponding curve in Figures 1 through 3) and then one performs a reliability analysis for that value of the tendon area to obtain the corresponding probabilistic design point. One then obtains initial values for the load factors for that structure and response component by dividing the value of the response component at the probabilistic design point by its characteristic values; i.e.,

---

where $P_E=\frac{2E}{1-\nu^2}\left(\frac{\tau}{D}\right)^3$, $P_0=2(\phi_y F_c)\left(\frac{\tau}{D}\right)$, E is Youngs' modulus, $\nu$ is Poisson's ratio and $(D/\tau)$ is the tendon diameter/thickness ratio. The bending capacity $F_b(\phi_y F_y)$ is calculated as

$$F_b=[\phi_y F_a]\left[(4/\pi)(1+\tau/D)-(0.006D/\tau)\right]$$

Source: R. Rashedi, Conoco, written communications to G. R. Toro, May 19, 1992, and July 20, 1992.

[8]The other $\gamma$ factors in Equation 3 are determined in the calibration of maximum offset, to be presented later.

[9]The choice of objective function to minimize is arbitrary. Another commonly used objective function is written in terms of differences of logarithms of the failure probabilities; this form and the form used here generally lead to similar results (Thoft-Christiansen and Baker, 1982). An objective function in terms of differences of failure probabilities would not be desirable because the calibration would be controlled by a few designs.

$$\gamma_i = \frac{X^*_i}{X_{c,i}} \tag{5}$$

Capacity factors for the axial capacity ($\phi_y$) are obtained by dividing the axial capacity at the design point by the nominal axial capacity. The resulting capacity factor is greater than one because of the assumed 15% bias in axial capacity. For the hydrostatic and bending capacities, the capacity factors are obtained as the ratio of the capacity at the design point by the capacity associated with the factored axial capacity $\phi_y F_a$ .[10]

Tables 5 and 6 show the initial load and capacity factors calculated in this manner, for safety indices of 3 and 4 [11]. These tables indicate that these factors are quite stable across the various TLP's. The average values over all structures (see Tables 5 and 5) serve as initial values of the partial safety factors. Finally, the initial values of the load factors are refined manually, so as to minimize the quantity

$$[mean\text{-}square\ residual]^2 = \frac{1}{n}\sum_{j=1}^{n} [\beta_j(\underline{\gamma},\underline{\phi}) - \beta_{target}]^2 \tag{6}$$

where the summation extends over all TLPs, $\beta_j(\underline{\gamma},\underline{\phi})$ is the safety index obtained for platform j, for given values of the load and capacity factors.

Figures 4 and 5 show the safety indices obtained using the initial values of the load and capacity factors. These figures show that the initial factors lead to safety indices higher than the target safety indices. This is caused by the simplified treatment of temporal and directional load combinations in the design equations, as follows: (1) the exact peak factors at the design point (approx. 3.5) is different from the peak factors used in the design equations ($[2\ln(n_i)]^{1/2}$; up to 3.7); (2) the design equation assumes that the wind, waves, and current are in line with each other and in line with a column diagonal[12]; and (3) the design equation uses the sum of the peak tensile and bending stresses (i.e., it assumes that both peaks occur at the same times).

---

[10] In the reliability calculations for this Section, the dependence among the three capacities is modeled in an approximate manner by introducing correlation among these quantities. This correlation was ignored in the first phase of this study.

[11] The anomalous factors for low-frequency wind ($X_{lfw}$) in 1000 m water depths are caused by problems in the depth scaling. These problems were later resolved and revised models for $X_{lfw}$ were used in the calibration of offset and air gap.

[12] The most exposed column diagonal is assumed to have an East-West direction, as was done in Phase I. This direction makes an angle of approximately 15 degrees with the mean wave direction. Changing the direction of the most exposed column diagonal so that it is the same as the mean wave direction causes a ≈10% increase in maximum tension for a given exceedance probability (see Phase-I report).

In the manual calibration, we adjust the load factors for setdown tension, static moment-induced tension, dynamic tension, and the factor $\gamma_{Xmax}$ in Equation 3, in order to minimize the quantity in Equation 6. We adjust $\gamma_{dyn}$ rather than the factors for the individual dynamic tensions for reasons of convenience and because the need for manual calibration arises from issues of dynamic load combination. Parameters such as $\gamma_{sd}$ and $\gamma_{mom}$, for which initial estimates are available in Tables 5 and 6, are varied within a $\sigma$ range; other parameters such as $\gamma_{dyn}$ and $\gamma_{Xmax}$ are initially set to their implied value of 1 and are varied over a wider range. The capacity factors are kept at their initial values.

The optimization is performed as follows.

1. For a given set of factors ($\gamma$), the factored tension and offset are calculated for each platform using Equations 2 and 3.

2. Each platform's tendons are designed (i.e., the required tendon area is calculated) using Equation 4.

3. The safety index $\beta_i(\gamma)$ for each platform is calculated (given the tendon area) for each platform, and the objective function in Equation 6 is evaluated. We also calculate the gradient of the objective function with respect to the load factors, in order to guide the selection of new values for the load factors.

4. New values of the load factors are selected (while staying within the ranges described above), and the process is repeated until there is no significant improvement in the objective function. The resulting load factors are referred to as the final or optimized load factors.

Tables 7 and 8 show the initial and optimized load and capacity factors and the associated mean-square $\beta$ residuals[13]. Figures 6 and 7 show the safety indices obtained using the optimized factors[14] and indicate a low scatter in the safety indices of platforms designed using the design equations and the factors developed here. Figure 8 shows the results for a safety index of 4 in a different form; namely, the ratio of steel tonnage of tendons sized according to the design equation to the tonnage of platforms sized using a probabilistic design (i.e., tendons that have safety indices identical to $\beta_{target}$).

Tables 7 and 8 (especially Table 8) show that the load factors vary significantly among themselves. This is because each response component has a different dependence on $H_S$. Static and second-order response components have much higher load factors than the first-order responses because the former are proportional to $H_S^2$, $V_W^2$, or $V_C^2$ (i.e., drag-type), while the

[13]The factors for the components of offset (Equation 3) are not shown. Recall that these factors take the values obtained in the calibration of offset (Tables 11 and 13) and are not varied as part of the tendon-design calibration.

[14]These figures are labeled "Case 2b" or "Case 3b" in the figure header.

latter are proportional to $H_S$ (i.e., inertia-type). In spite of this, the optimized coefficients lead to consistent safety indices.

In addition to the results in Tables 7 and 8, optimizations were performed assuming that all load factors in Equations 2 and 3 are equal (with the exception of $\gamma_{dyn,Tension}$, $\gamma_{Xmax}$, and $\gamma_{dyn,Xmax}$, which are set to 1). The calculated residual mean square is 0.10 for $\beta$=3 and 0.16 for $\beta$=4. The larger mean square obtained for $\beta$=4 indicates that the benefit of using multiple load factors. Another, perhaps more important, benefit of using multiple load factors is that the calibrated design equation is more stable with respect to changes in the characteristic environment or in platform configuration.

## Table 5

Initial Load and Capacity Factors for Tension Capacity (beta=3)

| TLP | Case | Xs | X1v | Xlfw | X2v | Tsd | Tm | T1v | T2v | Tw-sp | Fac | Fbc | Pc |
|---|---|---|---|---|---|---|---|---|---|---|---|---|---|
| GMS | *1.00 | 1.23 | 1.02 | 1.12 | 1.04 | 1.51 | 1.17 | 1.04 | 1.19 | 1.16 | 1.08 | 0.99 | 0.92 |
| GMS | *1.05 | 1.24 | 1.02 | 1.13 | 1.05 | 1.56 | 1.18 | 1.04 | 1.20 | 1.18 | 1.08 | 0.99 | 0.91 |
| GMS | *1.15 | 1.20 | 1.01 | 1.10 | 1.03 | 1.42 | 1.14 | 1.03 | 1.15 | 1.14 | 1.07 | 1.00 | 0.90 |
| GMS | *1.25 | 1.19 | 1.01 | 1.11 | 1.03 | 1.43 | 1.14 | 1.03 | 1.16 | 1.15 | 1.06 | 1.00 | 0.87 |
| GMS | 250 m | 1.28 | 1.04 | 1.24 | 1.07 | 1.67 | 1.21 | 1.05 | 1.26 | 1.21 | 1.08 | 0.99 | 0.94 |
| GMS | 500 m | 1.24 | 1.02 | 1.14 | 1.05 | 1.55 | 1.18 | 1.04 | 1.20 | 1.17 | 1.08 | 0.99 | 0.92 |
| GMS | 1000 m | 1.17 | 0.98 | 1.02 | 1.02 | 1.38 | 1.10 | 1.00 | 1.09 | 1.09 | 1.09 | 0.99 | 0.94 |
| NSS | *0.75 | 1.32 | 1.07 | 1.39 | 1.05 | 1.75 | 1.27 | 1.06 | 1.28 | 1.26 | 1.09 | 0.98 | 0.95 |
| NSS | *0.85 | 1.30 | 1.06 | 1.32 | 1.05 | 1.64 | 1.25 | 1.06 | 1.28 | 1.25 | 1.08 | 0.98 | 0.95 |
| NSS | *0.95 | 1.27 | 1.06 | 1.26 | 1.05 | 1.56 | 1.24 | 1.06 | 1.26 | 1.22 | 1.07 | 0.99 | 0.95 |
| NSS | *1.00 | 1.25 | 1.06 | 1.24 | 1.04 | 1.63 | 1.22 | 1.06 | 1.24 | 1.21 | 1.06 | 0.99 | 0.95 |
| NSS | *1.05 | 1.23 | 1.05 | 1.21 | 1.05 | 1.59 | 1.21 | 1.05 | 1.23 | 1.20 | 1.05 | 0.99 | 0.95 |
| NSS | *1.15 | 1.19 | 1.04 | 1.16 | 1.03 | 1.00 | 1.18 | 1.04 | 1.19 | 1.17 | 1.04 | 0.99 | 0.95 |
| NSS | *1.25 | 1.16 | 1.03 | 1.14 | 1.03 | 1.50 | 1.15 | 1.04 | 1.15 | 1.15 | 1.03 | 1.00 | 0.95 |
| NSS | 500 m | 1.23 | 1.03 | 0.95 | 1.03 | 1.50 | 1.19 | 1.04 | 1.18 | 1.18 | 1.07 | 0.99 | 0.95 |
| NSS | 1000 m | 1.22 | 1.01 | 0.93 | 1.02 | 1.49 | 1.17 | 1.03 | 1.15 | 1.16 | 1.07 | 1.00 | 0.94 |
| NSC | *0.75 | 1.26 | 1.03 | 1.20 | 1.04 | 1.61 | 1.21 | 1.03 | 1.20 | 1.21 | 1.08 | 0.99 | 0.95 |
| NSC | *0.85 | 1.25 | 1.04 | 1.16 | 1.04 | 1.58 | 1.20 | 1.04 | 1.21 | 1.21 | 1.08 | 0.99 | 0.94 |
| NSC | *0.95 | 1.25 | 1.05 | 1.16 | 1.04 | 1.63 | 1.22 | 1.05 | 1.22 | 1.22 | 1.07 | 0.99 | 0.93 |
| NSC | *1.00 | 1.26 | 1.05 | 1.16 | 1.04 | 1.63 | 1.22 | 1.05 | 1.23 | 1.22 | 1.06 | 0.99 | 0.93 |
| NSC | 500 m | 1.21 | 1.02 | 1.06 | 1.03 | 1.55 | 1.17 | 1.03 | 1.16 | 1.18 | 1.07 | 1.00 | 0.91 |
| NSC | 1000 m | 1.19 | 0.98 | 0.98 | 1.01 | 1.41 | 1.13 | 1.01 | 1.11 | 1.13 | 1.08 | 1.00 | 0.92 |
| AVG. | | 1.23 | 1.03 | 1.15 | 1.04 | 1.53 | 1.19 | 1.04 | 1.20 | 1.19 | 1.07 | 0.99 | 0.93 |
| C.O.V | | 0.03 | 0.02 | 0.10 | 0.01 | 0.10 | 0.04 | 0.01 | 0.04 | 0.03 | 0.01 | 0.01 | 0.02 |

## Table 6

Initial Part. Load and Capacity Factors for Tendon Capacity (beta=4)

| TLP | Case | Xs | X1v | X1fw | X2v | Tsd | Tm | T1v | T2v | Tw-sp | Fy | Fb | Pc |
|---|---|---|---|---|---|---|---|---|---|---|---|---|---|
| GMS | *1.00 | 1.90 | 1.31 | 1.46 | 1.24 | 3.58 | 1.85 | 1.26 | 2.01 | 1.83 | 1.05 | 0.99 | 0.92 |
| GMS | *1.05 | 1.90 | 1.32 | 1.48 | 1.25 | 3.67 | 1.85 | 1.27 | 2.06 | 1.84 | 1.04 | 0.99 | 0.92 |
| GMS | *1.15 | 1.89 | 1.33 | 1.50 | 1.27 | 3.58 | 1.85 | 1.27 | 2.09 | 1.83 | 1.04 | 0.99 | 0.90 |
| GMS | *1.25 | 1.89 | 1.34 | 1.53 | 1.28 | 3.59 | 1.83 | 1.27 | 2.13 | 1.82 | 1.03 | 0.99 | 0.88 |
| GMS | 250 m | 1.99 | 1.33 | 1.90 | 1.26 | 4.00 | 1.89 | 1.28 | 2.16 | 1.88 | 1.04 | 0.98 | 0.95 |
| GMS | 500 m | 1.91 | 1.31 | 1.51 | 1.24 | 3.68 | 1.86 | 1.27 | 2.04 | 1.84 | 1.05 | 0.99 | 0.93 |
| GMS | 1000 m | 1.80 | 1.28 | 1.06 | 1.22 | 3.25 | 1.77 | 1.23 | 1.86 | 1.76 | 1.05 | 0.99 | 0.97 |
| NSS | *0.75 | 2.11 | 1.38 | 1.96 | 1.15 | 4.42 | 2.00 | 1.29 | 2.10 | 1.99 | 1.04 | 0.96 | 0.99 |
| NSS | *0.85 | 2.10 | 1.41 | 1.88 | 1.22 | 4.36 | 2.02 | 1.30 | 2.27 | 2.00 | 1.04 | 0.97 | 0.99 |
| NSS | *0.95 | 2.09 | 1.44 | 1.82 | 1.27 | 4.31 | 2.02 | 1.31 | 2.37 | 1.99 | 1.03 | 0.98 | 0.98 |
| NSS | *1.00 | 2.06 | 1.45 | 1.80 | 1.26 | 4.44 | 2.00 | 1.31 | 2.40 | 1.98 | 1.02 | 0.98 | 0.98 |
| NSS | *1.05 | 2.04 | 1.46 | 1.77 | 1.29 | 4.35 | 1.98 | 1.30 | 2.40 | 1.98 | 1.01 | 0.99 | 0.98 |
| NSS | *1.15 | 1.98 | 1.48 | 1.74 | 1.29 | 3.50 | 1.94 | 1.30 | 2.38 | 1.93 | 1.00 | 0.99 | 0.98 |
| NSS | *1.25 | 1.91 | 1.48 | 1.70 | 1.30 | 4.00 | 1.88 | 1.29 | 2.31 | 1.86 | 0.99 | 0.99 | 0.98 |
| NSS | 500 m | 1.97 | 1.41 | 0.79 | 1.26 | 3.77 | 1.93 | 1.28 | 2.16 | 1.92 | 1.04 | 0.99 | 0.97 |
| NSS | 1000 m | 1.87 | 1.37 | 0.76 | 1.24 | 3.46 | 1.86 | 1.25 | 1.97 | 1.85 | 1.04 | 0.99 | 0.96 |
| NSC | *0.75 | 1.96 | 1.38 | 1.45 | 1.08 | 3.86 | 1.94 | 1.26 | 1.80 | 1.94 | 1.05 | 0.98 | 0.95 |
| NSC | *0.85 | 1.96 | 1.42 | 1.45 | 1.16 | 3.84 | 1.94 | 1.27 | 1.98 | 1.96 | 1.04 | 0.99 | 0.95 |
| NSC | *0.95 | 1.97 | 1.46 | 1.47 | 1.21 | 3.88 | 1.95 | 1.27 | 2.10 | 1.96 | 1.04 | 0.99 | 0.94 |
| NSC | *1.00 | 1.98 | 1.48 | 1.48 | 1.23 | 4.00 | 1.94 | 1.28 | 2.14 | 1.95 | 1.04 | 0.99 | 0.93 |
| NSC | 500 m | 1.92 | 1.46 | 1.16 | 1.23 | 4.00 | 1.90 | 1.27 | 2.04 | 1.92 | 1.04 | 0.99 | 0.92 |
| NSC | 1000 m | 1.84 | 1.40 | 0.87 | 1.21 | 3.36 | 1.82 | 1.24 | 1.87 | 1.83 | 1.04 | 1.00 | 0.94 |
| AVG. | | 1.96 | 1.40 | 1.48 | 1.23 | 3.87 | 1.91 | 1.28 | 2.13 | 1.91 | 1.03 | 0.99 | 0.95 |
| C.O.V | | 0.04 | 0.04 | 0.24 | 0.04 | 0.09 | 0.04 | 0.02 | 0.08 | 0.04 | 0.01 | 0.01 | 0.03 |

**Table 7**
Load and Capacity Factors for
Tendon Capacity
beta=3

| Factor | Initial | Optimized |
|---|---|---|
| Tsd | 1.53 | 1.40 |
| Tmom | 1.19 | 1.20 |
| Tdyn | 1.00 | 0.80 |
| T1v | 1.04 | 1.04 |
| T2v | 1.20 | 1.20 |
| Tws-p | 1.19 | 1.19 |
| Xmax | 1.00 | 0.70 |
| Fy | 1.07 | 1.07 |
| Fb | 0.99 | 0.99 |
| Pc | 0.93 | 0.93 |
| residual mean square | 0.35 | 0.09 |

**Table 8**
Load and Capacity Factors for
Tendon Capacity
(beta=4)

| Factor | Initial | Optimized |
|---|---|---|
| Tsd | 3.87 | 3.50 |
| Tmom | 1.91 | 1.80 |
| Tdyn | 1.00 | 0.85 |
| T1v | 1.28 | 1.28 |
| T2v | 2.13 | 2.13 |
| Tws-p | 1.91 | 1.91 |
| Xmax | 1.00 | 0.70 |
| Fy | 1.03 | 1.03 |
| Fb | 0.99 | 0.99 |
| Pc | 0.93 | 0.93 |
| residual mean square | 0.35 | 0.09 |

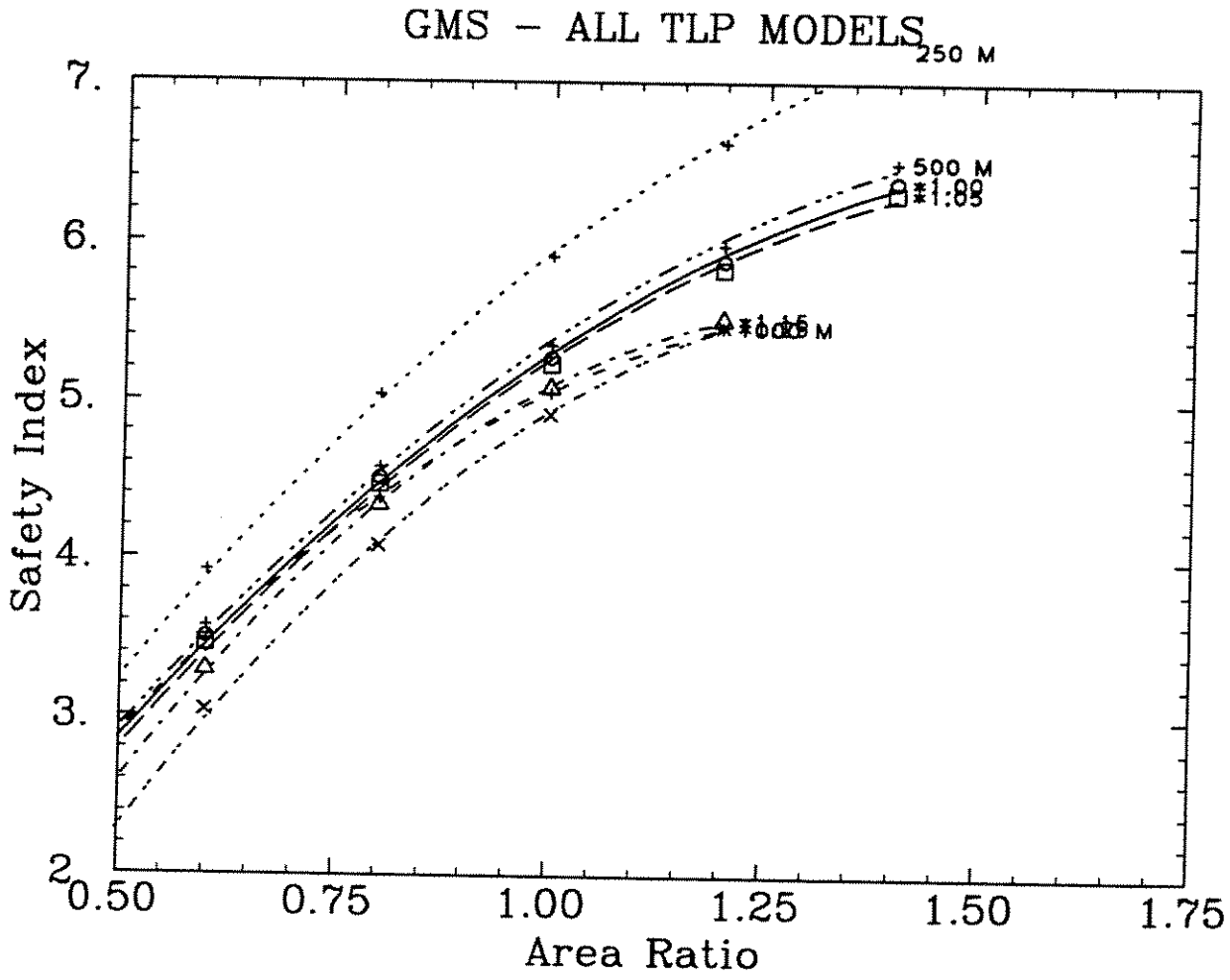


**Figure 1.** Variation of tendon safety index as a function of tendon cross-sectional area for all designs based on the GMS platform. An area ratio of 1 corresponds to the base tendon dimensions.

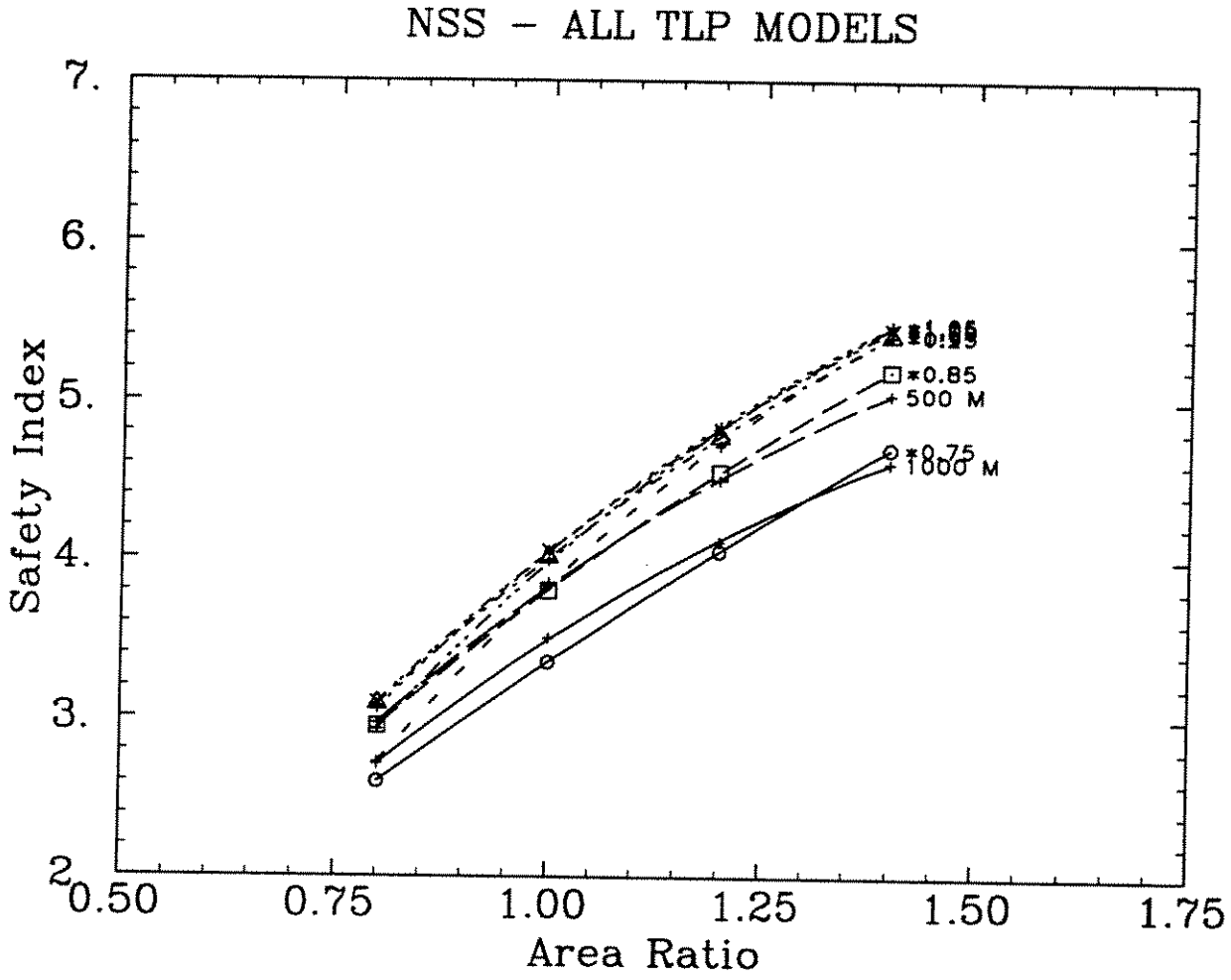


**Figure 2.** Variation of tendon safety index as a function of tendon cross-sectional area for all designs based on the NSS platform. An area ratio of 1 corresponds to the base tendon dimensions.

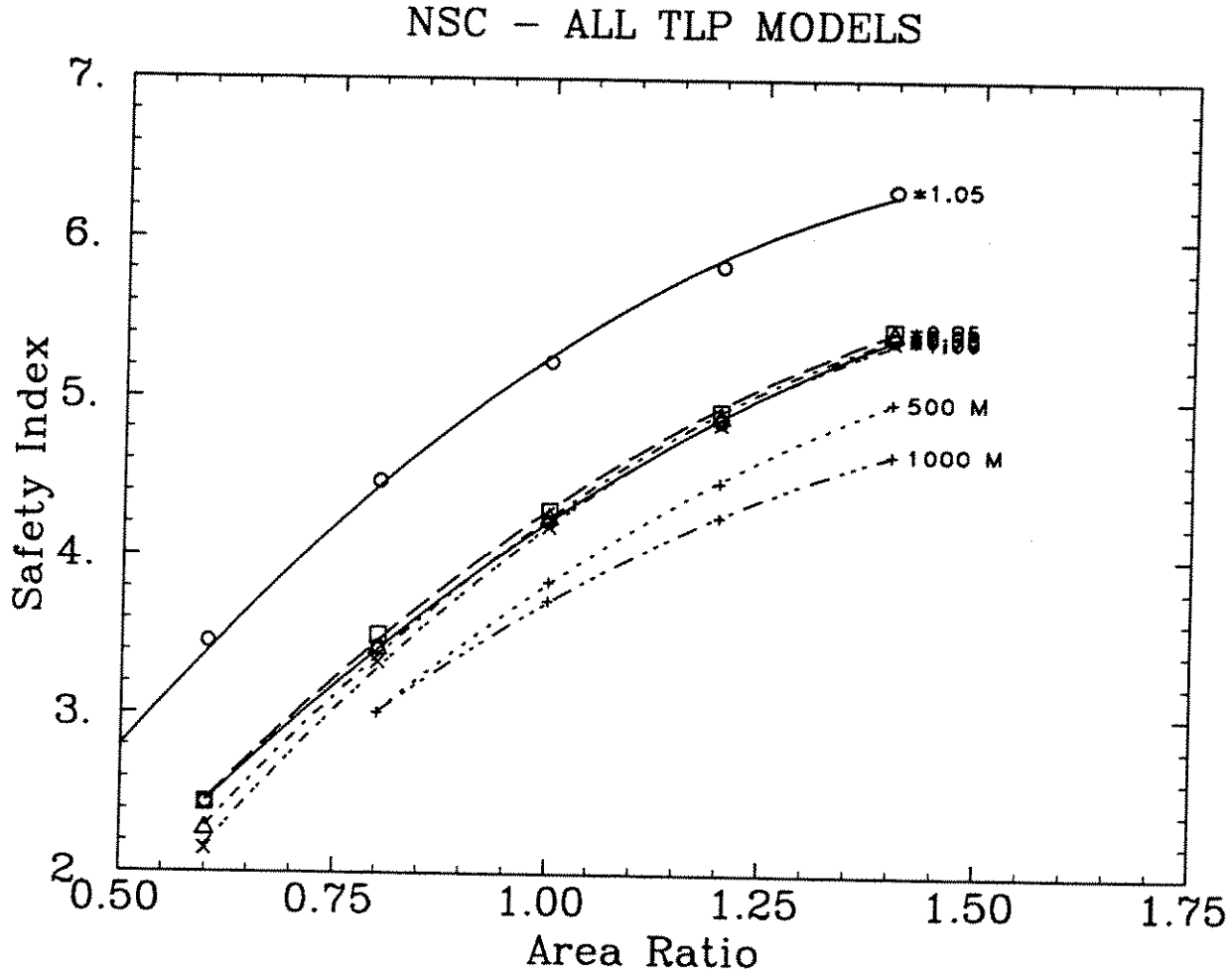


**Figure 3.** Variation of tendon safety as a function of tendon cross-sectional area for all designs based on the NSC platform. An area ratio of 1 corresponds to the base tendon dimensions.

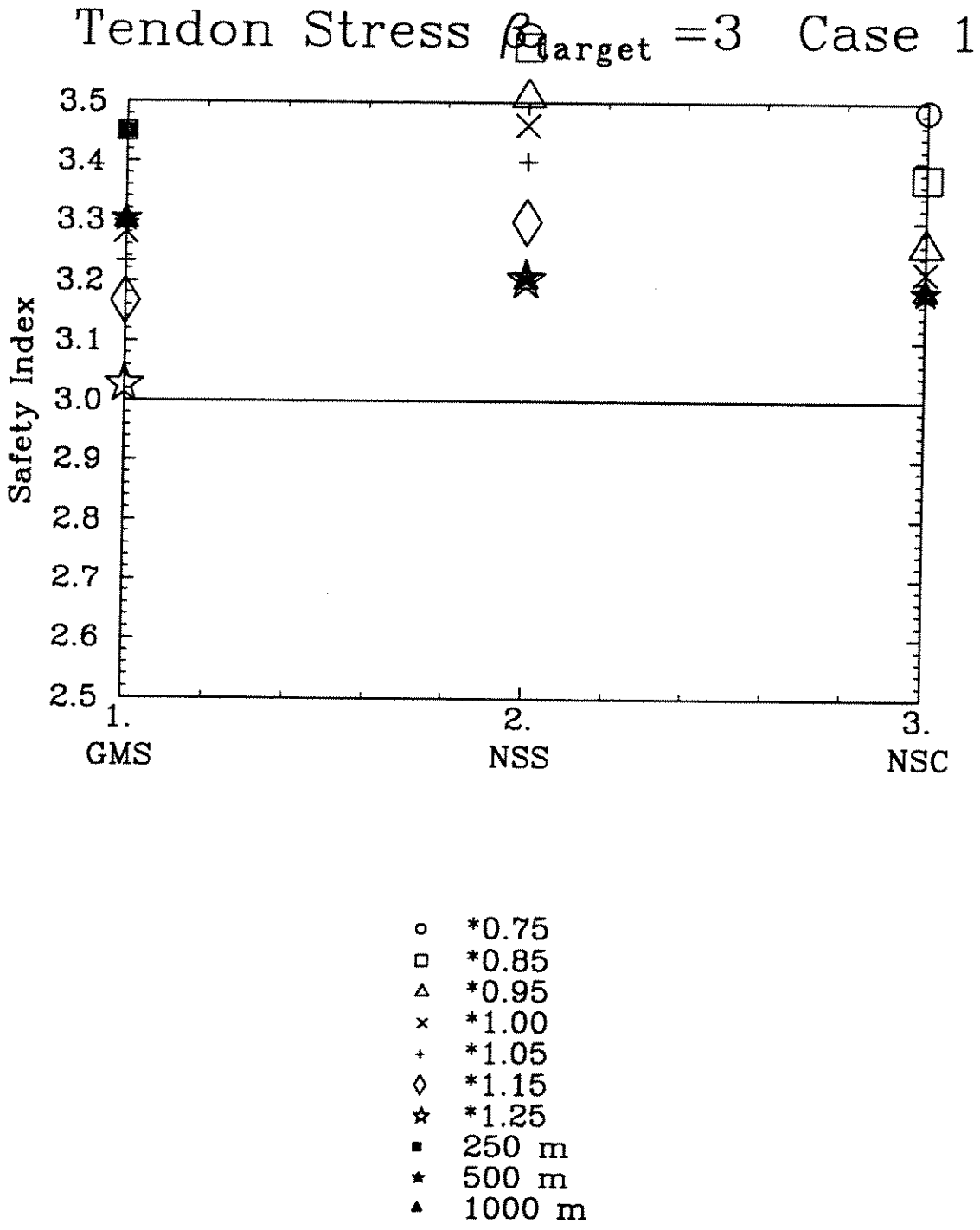


**Figure 4.** Safety indices for tendon capacity obtained using the initial load factors; target safety index: 3.

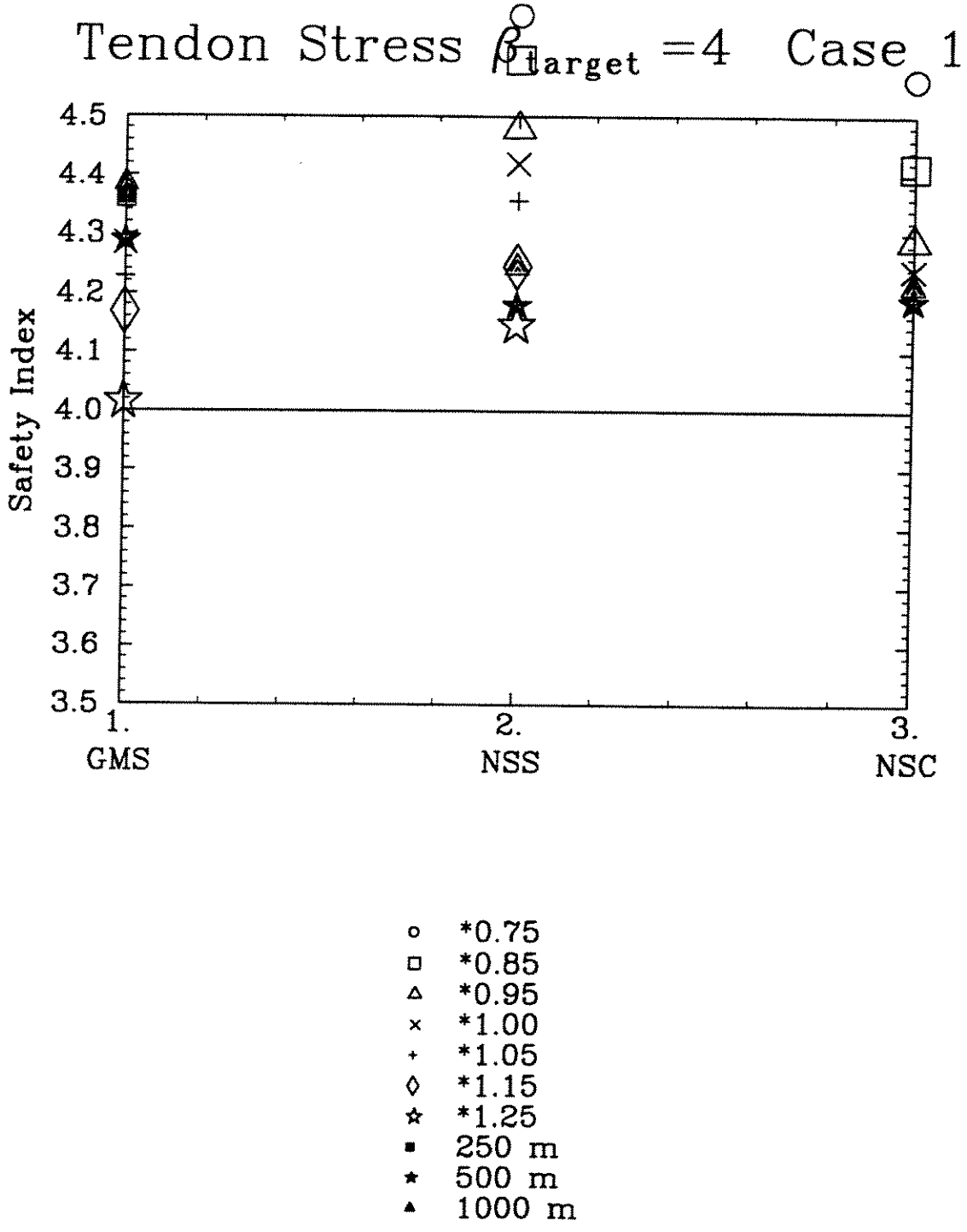


**Figure 5.** Safety indices for tendon capacity obtained using the initial load factors; target safety index: 4.

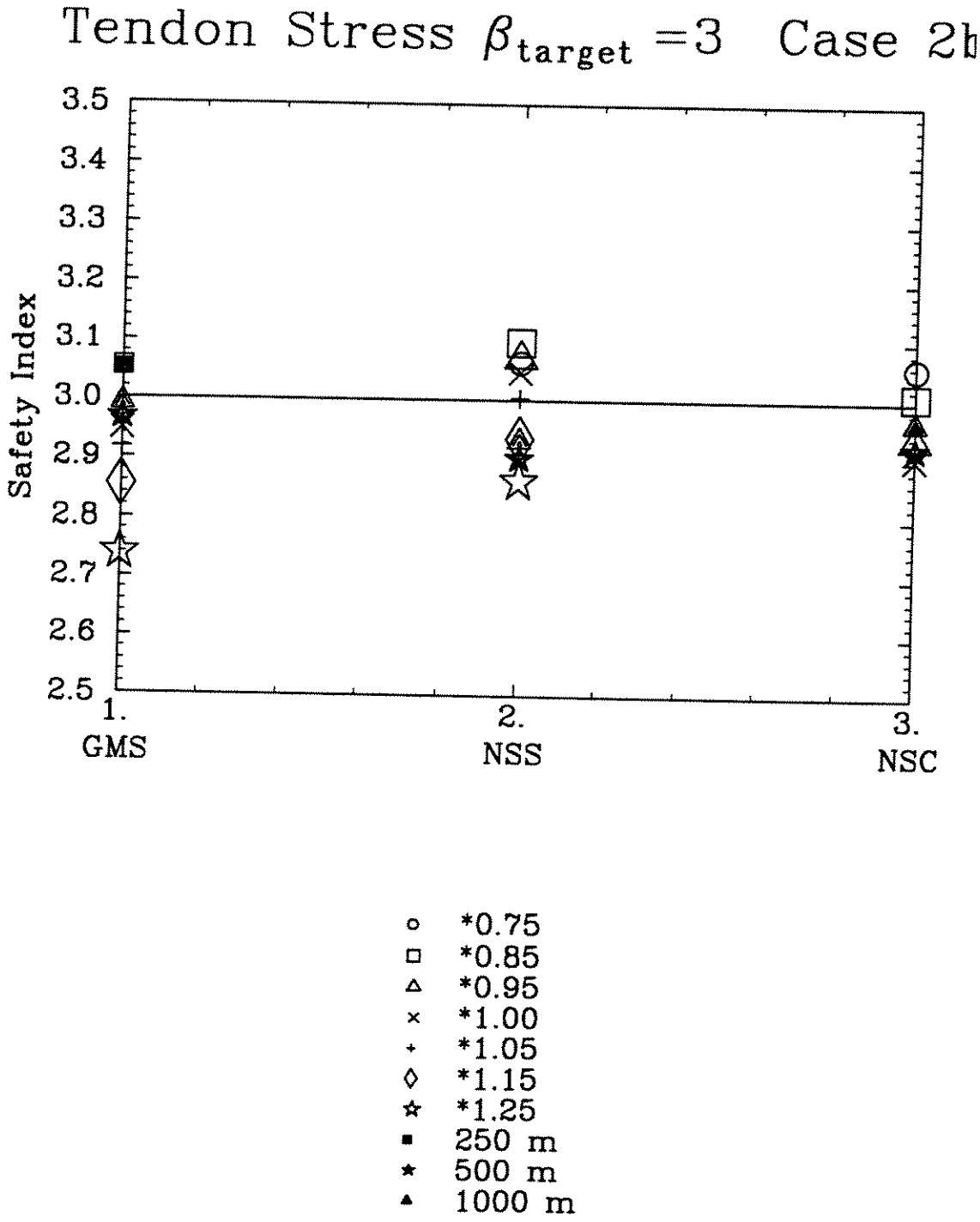


**Figure 6.** Safety indices for tendon capacity obtained using the optimized load factors; target safety index: 3.

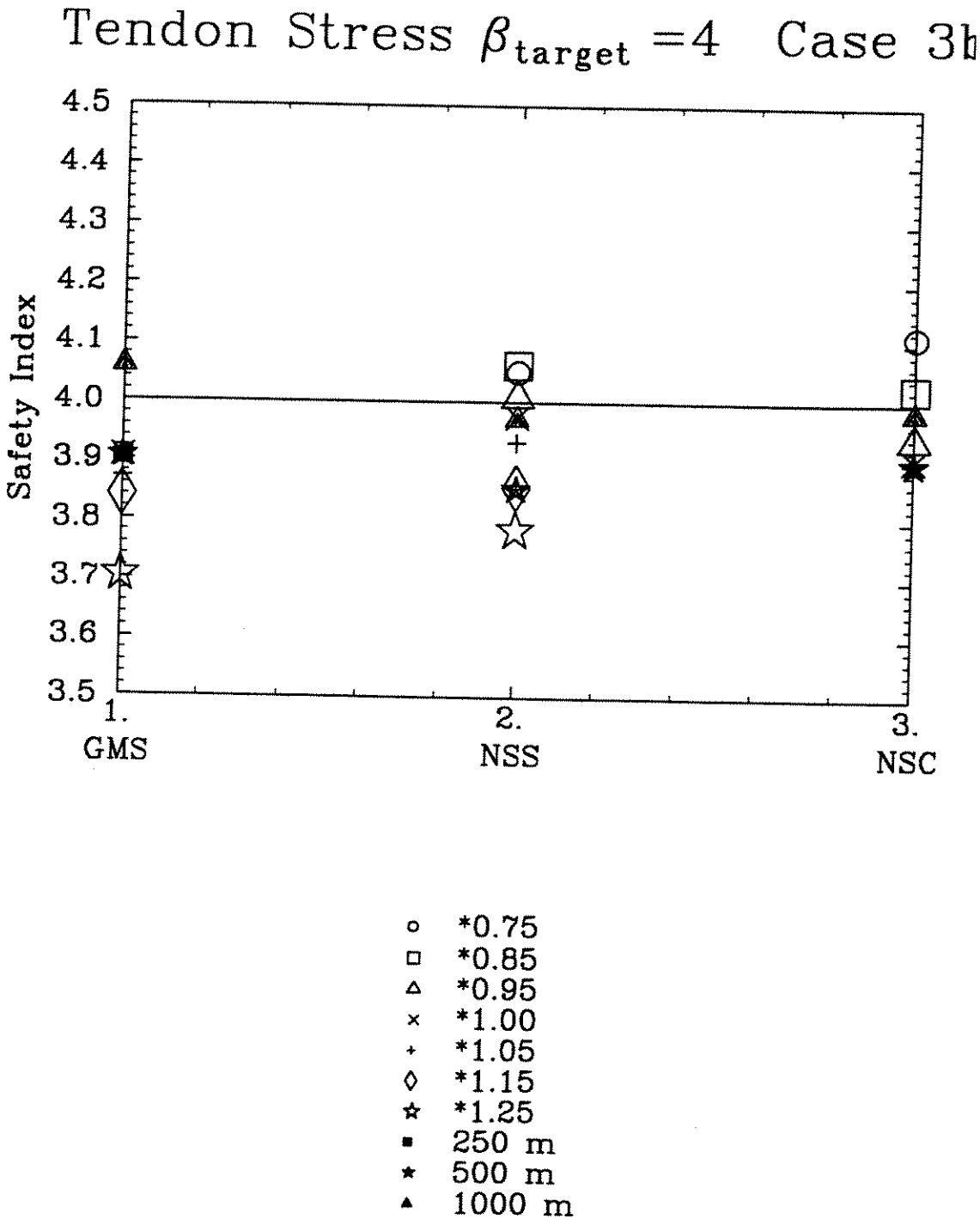


**Figure 7.** Safety indices for tendon capacity obtained using the optimized load factors; target safety index: 4.

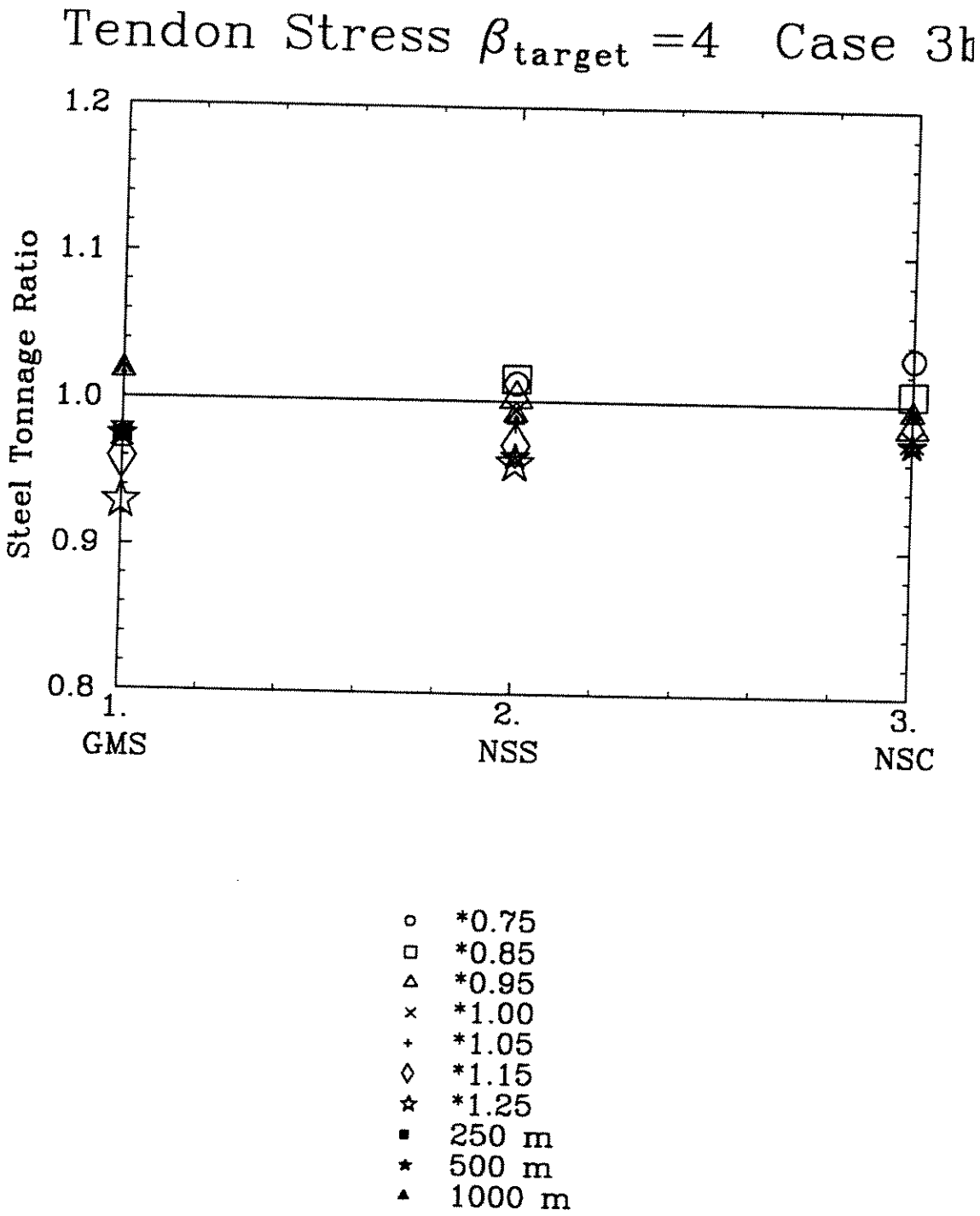


**Figure 8.** Ratio of steel tonnage (tendon designed using load factors/probabilistic design); Target safety index: 4.

## CALIBRATION FOR MAXIMUM OFFSET

The calibration of maximum offset, minimum tension, and air gap is slightly different from that of tendon capacity in that no "design" is involved. The approach followed here is to develop load factors such that the global response calculated using those factors has a probability of exceedance (as represented by the safety index) as close as possible to the target exceedance probability. To this effect, we minimize the quantity

$$[mean\text{-}square\ residual]^2=\frac{1}{n}\sum_{j=1}^{n}\left[\beta_j(\gamma)-\beta_{target}\right]^2 \tag{7}$$

where $\beta_j(\gamma)$ is the safety index corresponding to the probability of exceeding the maximum offset calculated with the equation

$$X_{\max}=\gamma_s X_s+\gamma_{dyn}\left\{\sum_i (B_i\gamma_i X_i)^2\right\}^{1/2} \tag{8}$$

where the X's represent characteristic values of the various components of offset and the $\gamma_i$'s and $B_i$ represent load factors and peak factors. $X_s$ is the static offset (due to mean wind, current, and wave-drift forces), and the $X_i$'s represent rms values of dynamic components of offsets, as follows: first-order wave-frequency offset $X_{1v}$, (2) second-order low-frequency wave-induced offset $X_{2v}$, and (3) low-frequency wind-induced offset $X_{lfw}$.

Calibration is performed for safety indices of 3, 3.5, and 4 [15]. Tables 9 and 10 show the calculation of initial partial load factors for offset; these factors are quite stable across the various TLP's and scaling factors. Figures 9 and 10 show the safety indices associated with the initial values of load factors[16]. Unlike the tendon capacity results, these figures do not indicate a tendency to higher safety indices (which would correspond to overestimation of offsets).

We adjust the factors for the static offset and the combined dynamic offsets. The final values of factors $\gamma_s$ (static offset) and $\gamma_{dyn}$ are within 10 and 15 percent of their initial values, respectively. Tables 11 through 13 show the initial and optimized factors for safety indices of 3, 3.5, and 4. Figures 11 and 12 show the actual safety indices associated with the load factors, for target safety indices of 3 and 3.5. These figures show a small scatter about the target $\beta$'s, indicating that the calculated load factors for offset result in accurate estimates of the offset associated with the target safety index.

---

[15]Calibration for $\beta$=4 is required because these offset coefficients are used in the calibration of tendon capacity and air gap (see Eqs. 3 and 10).

[16]i.e., the safety indices associated with maximum offsets calculated using the initial load factors.

**Table 9**
Initial Load and Capacity Factors
for Offset (beta=3)

| TLP | Case | Xs | X1v | Xlfw | X2v |
|---|---|---|---|---|---|
| GMS | *1.00 | 1.31 | 1.02 | 1.26 | 1.07 |
| GMS | *1.05 | 1.31 | 1.02 | 1.26 | 1.07 |
| GMS | *1.15 | 1.31 | 1.02 | 1.26 | 1.07 |
| GMS | *1.25 | 1.31 | 1.02 | 1.27 | 1.07 |
| GMS | 250 m | 1.37 | 1.06 | 1.42 | 1.10 |
| GMS | 500 m | 1.31 | 1.02 | 1.31 | 1.07 |
| GMS | 1000 m | 1.23 | 0.98 | 1.72 | 1.04 |
| NSS | *0.75 | 1.43 | 1.11 | 1.66 | 1.05 |
| NSS | *0.85 | 1.44 | 1.12 | 1.67 | 1.06 |
| NSS | *0.95 | 1.44 | 1.12 | 1.69 | 1.07 |
| NSS | *1.00 | 1.45 | 1.12 | 1.70 | 1.07 |
| NSS | *1.05 | 1.44 | 1.13 | 1.70 | 1.09 |
| NSS | *1.15 | 1.44 | 1.13 | 1.71 | 1.08 |
| NSS | *1.25 | 1.44 | 1.15 | 1.72 | 1.09 |
| NSS | 500 m | 1.35 | 1.06 | 1.48 | 1.04 |
| NSS | 1000 m | 1.28 | 1.01 | 1.33 | 1.02 |
| NSC | *0.75 | 1.41 | 1.10 | 1.64 | 1.02 |
| NSC | *0.85 | 1.42 | 1.11 | 1.65 | 1.05 |
| NSC | *0.95 | 1.43 | 1.13 | 1.66 | 1.06 |
| NSC | *1.00 | 1.44 | 1.13 | 1.67 | 1.07 |
| NSC | 500 m | 1.41 | 1.11 | 1.67 | 1.06 |
| NSC | 1000 m | 1.37 | 1.09 | 1.54 | 1.05 |
| AVG. | | 1.38 | 1.08 | 1.56 | 1.06 |
| C.O.V | | 0.05 | 0.05 | 0.11 | 0.02 |

**Table 10**
Initial Part. Load and Capacity Factors
for Offset (beta=3.5)

| TLP | Case | Xs | X1v | Xlfw | X2v |
|---|---|---|---|---|---|
| GMS | *1.00 | 1.70 | 1.19 | 1.57 | 1.20 |
| GMS | *1.05 | 1.71 | 1.19 | 1.58 | 1.21 |
| GMS | *1.15 | 1.72 | 1.20 | 1.60 | 1.22 |
| GMS | *1.25 | 1.73 | 1.21 | 1.62 | 1.23 |
| GMS | 250 m | 1.83 | 1.25 | 2.00 | 1.22 |
| GMS | 500 m | 1.71 | 1.20 | 1.80 | 1.19 |
| GMS | 1000 m | 1.60 | 1.15 | 2.31 | 1.16 |
| NSS | *0.75 | 1.84 | 1.28 | 2.12 | 1.10 |
| NSS | *0.85 | 1.86 | 1.29 | 2.18 | 1.15 |
| NSS | *0.95 | 1.87 | 1.31 | 2.22 | 1.17 |
| NSS | *1.00 | 1.88 | 1.32 | 2.24 | 1.19 |
| NSS | *1.05 | 1.89 | 1.34 | 2.26 | 1.20 |
| NSS | *1.15 | 1.89 | 1.37 | 2.29 | 1.21 |
| NSS | *1.25 | 1.89 | 1.39 | 2.32 | 1.23 |
| NSS | 500 m | 1.78 | 1.27 | 2.05 | 1.17 |
| NSS | 1000 m | 1.68 | 1.23 | 1.82 | 1.15 |
| NSC | *0.75 | 1.74 | 1.27 | 1.98 | 1.04 |
| NSC | *0.85 | 1.77 | 1.30 | 2.02 | 1.10 |
| NSC | *0.95 | 1.79 | 1.33 | 2.06 | 1.13 |
| NSC | *1.00 | 1.81 | 1.34 | 2.09 | 1.15 |
| NSC | 500 m | 1.77 | 1.35 | 2.30 | 1.15 |
| NSC | 1000 m | 1.72 | 1.33 | 2.12 | 1.15 |
| AVG. | | 1.79 | 1.28 | 2.05 | 1.17 |
| C.O.V | | 0.05 | 0.05 | 0.12 | 0.04 |

**Table 11**
Load and Capacity Factors
for Offset (beta=3)

| Factor | Initial | Optimized |
|---|---|---|
| Xs | 1.38 | 1.30 |
| Xdyn | 1.00 | 1.10 |
| X1v | 1.08 | 1.08 |
| X2v | 1.06 | 1.06 |
| Xlfw | 1.56 | 1.56 |
| residual mean square | 0.10 | 0.08 |

**Table 12**
Load and Capacity Factors
for Offset (beta=3.5)

| Factor | Initial | Optimized |
|---|---|---|
| Xs | 1.79 | 1.69 |
| Xdyn | 1.00 | 1.10 |
| X1v | 1.28 | 1.28 |
| X2v | 1.17 | 1.17 |
| Xlfw | 2.05 | 2.05 |
| residual mean square | 0.12 | 0.08 |

**Table 13**
Load and Capacity Factors
for Offset (beta=4)

| Factor | Initial | Optimized |
|---|---|---|
| Xs | 2.20 | 2.00 |
| Xdyn | 1.00 | 1.15 |
| X1v | 1.46 | 1.42 |
| X2v | 1.25 | 1.25 |
| Xlfw | 2.57 | 2.14 |
| residual mean square | 0.33 | 0.10 |

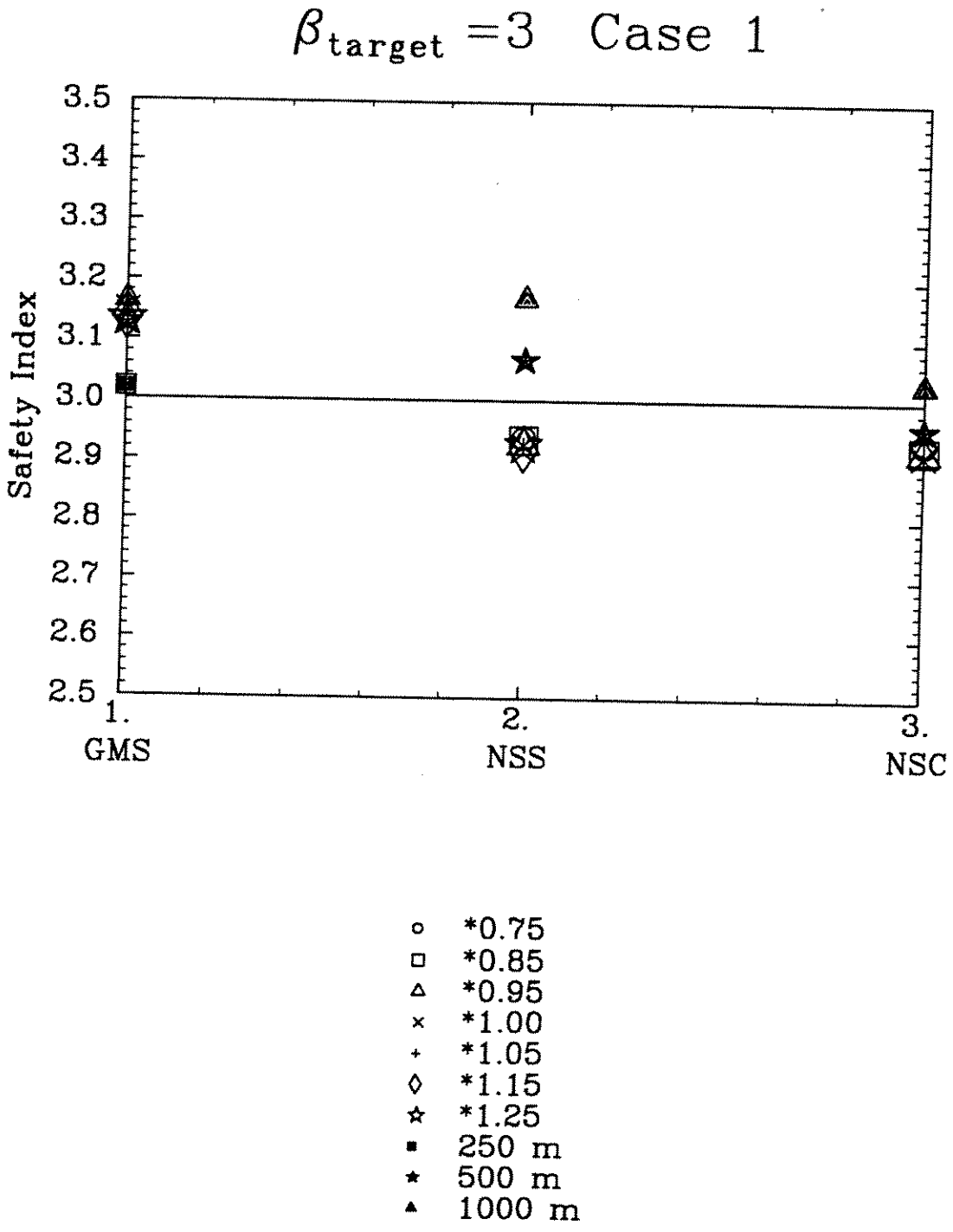


**Figure 9.** Safety indices for maximum offset obtained using the initial load factors; target safety index: 3.

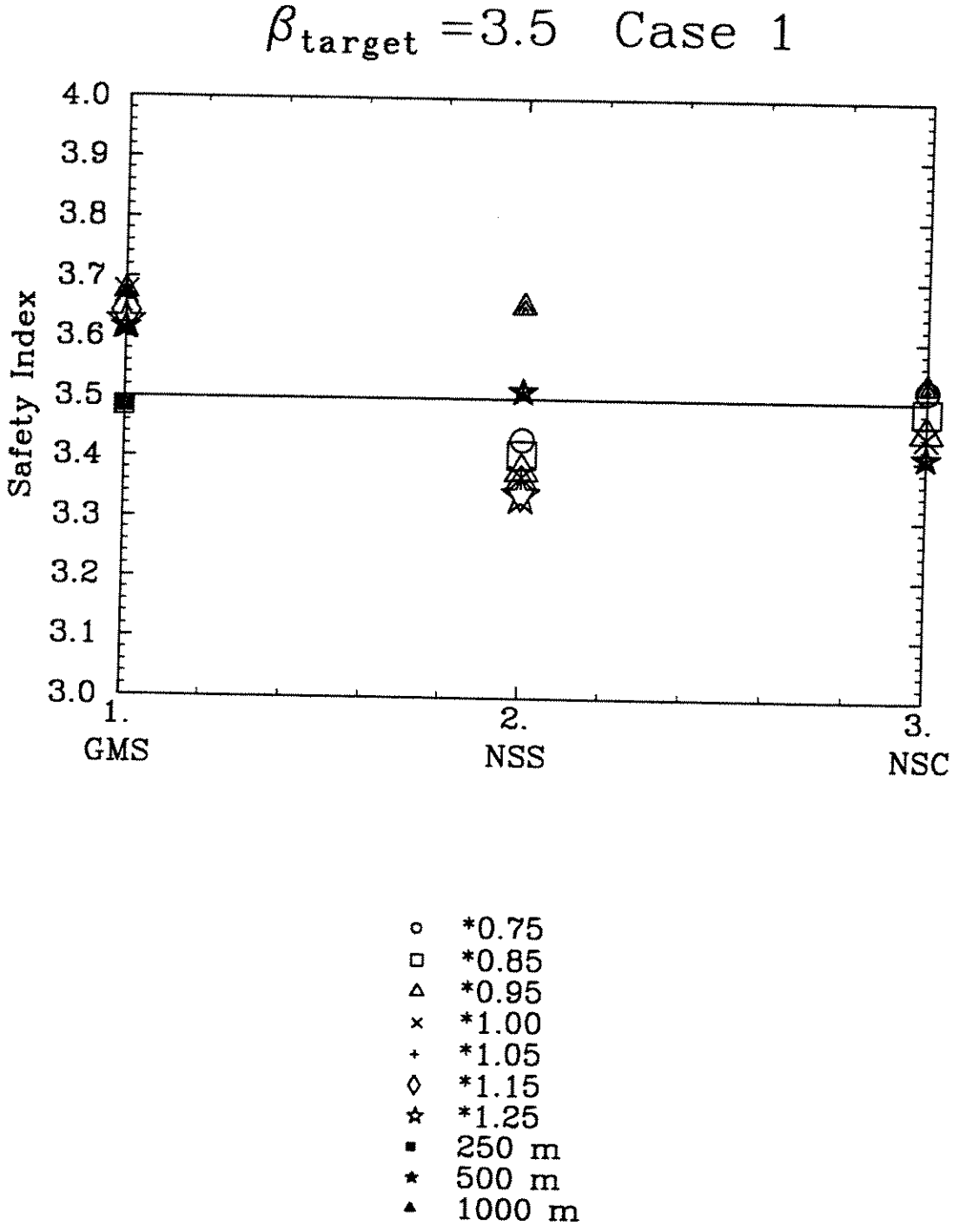


**Figure 10.** Safety indices for maximum offset obtained using the initial load factors; target safety index: 3.5.

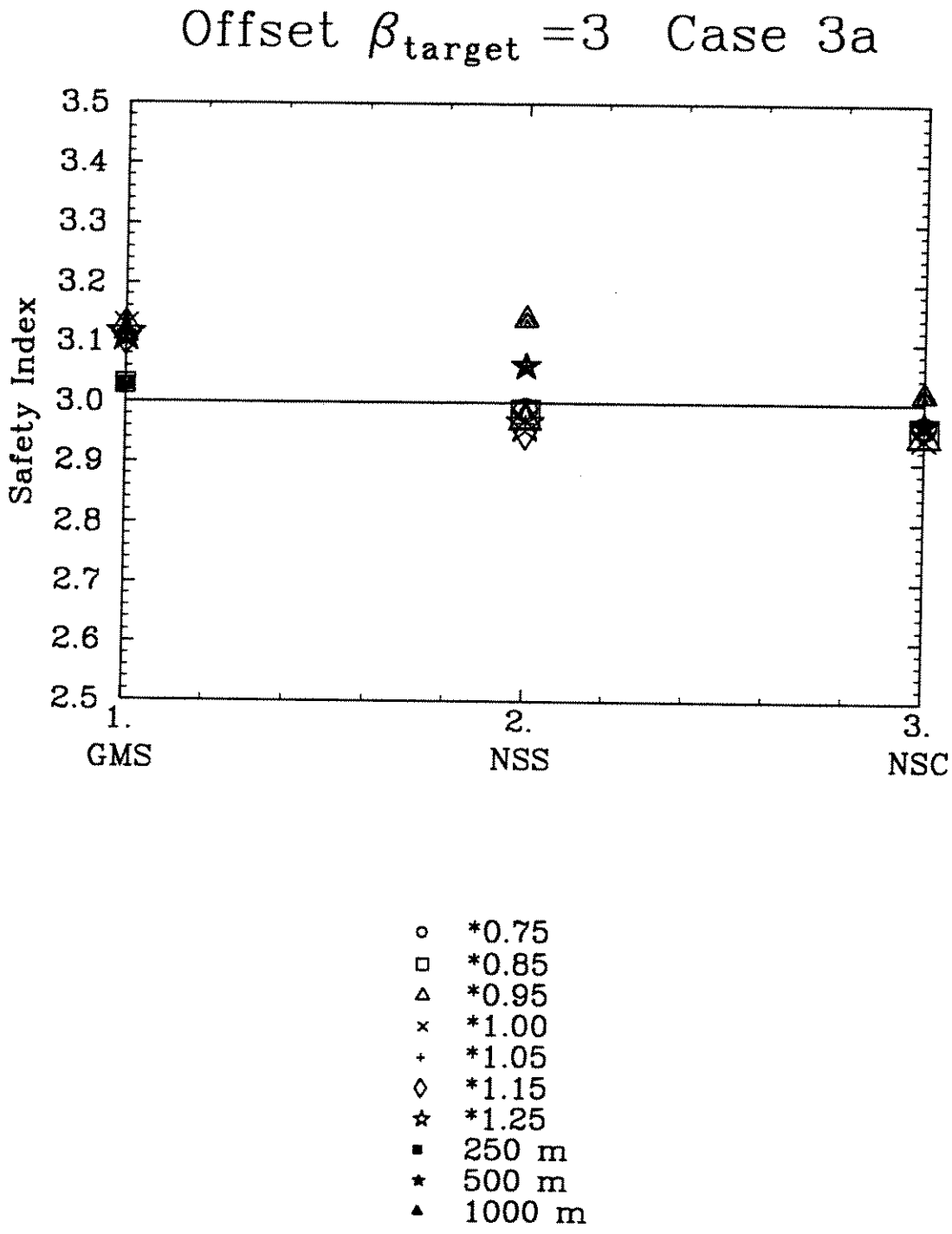


**Figure 11.** Safety indices for maximum offset obtained using the optimized load factors; target safety index: 3.

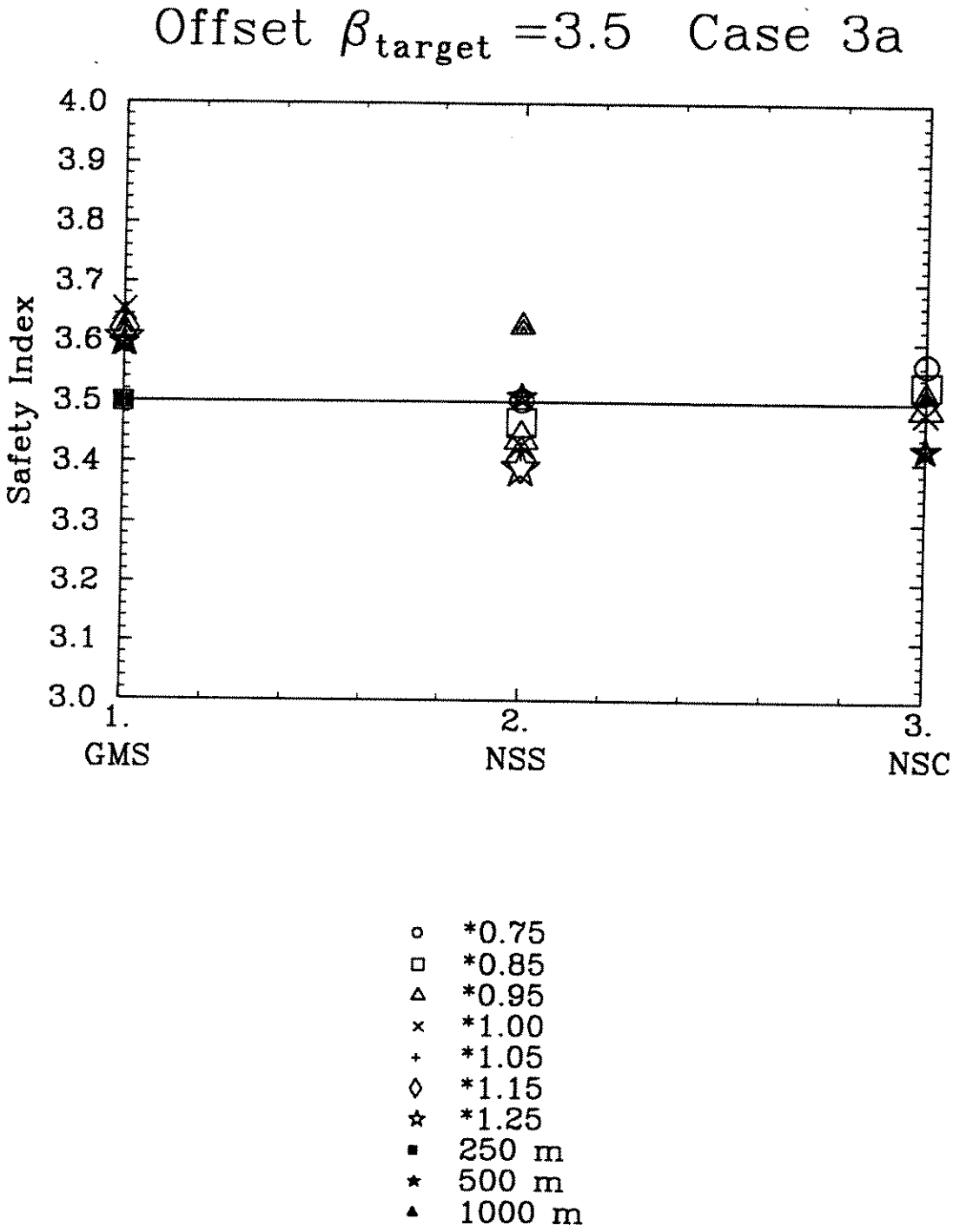


**Figure 12.** Safety indices for maximum offset obtained using the optimized load factors; target safety index: 3.5.

## CALIBRATION FOR MINIMUM TENSION

The calibration process for minimum tension is similar to that followed for maximum offset. The equation for the calculation of the minimum tension associated with a target safety index considers a down-weather tendon and has the form

$$T_{\min} = T_0 + \gamma_{sd} T_{sd} - \gamma_{mom} T_{mom} - \gamma_{dyn} \left\{ \sum_i (B_i \gamma_i T_i)^2 \right\}^{1/2} \tag{9}$$

where all terms have the same meaning as in Equation 2.

Tables 14 and 15 show the calculation of initial load factors. These tables indicate that the factors for setdown tension has much higher variability across platforms than the factors considered earlier. Platforms in deeper water show lower values than platforms in shallower water. This dependence on water depth is not caused by problems with scaling[17]. Rather, the low values of $\gamma_{sd}$ are an indication that setdown acts against minimum tension and is more important for platforms in deep water. The factor for static moment-induced tension shows a similar, but less pronounced, pattern.

Figures 13 and 14 show the safety indices associated with the initial load factors. These figures indicate that the initial factors are unconservative (i.e., they overestimate the minimum tension).

Adjustments in the load factor for setdown tension (see Tables 16 and 17) brings the safety index near the target safety index; the magnitude of the adjustment (up to 35 percent) is justified given the large variability across platforms. No adjustments to the other factors are required. Figures 15 and 16 show the safety indices associated with the final load factors. These figures show little scatter about the target $\beta$ for all platforms, indicating that the final load factors lead to accurate estimates of the minimum tension associated with the target load factor.

[17] The equations used in the static-offset calculations are based on equilibrium of the TLP hull, not on regressions. Thus, these equations are easily scaled.

**Table 14**
Initial Load and Capacity Factors
for Minimum Tension (beta=3)

| TLP | Case | Tsd | Tm | T1v | T2v | Tw-sp |
|---|---|---|---|---|---|---|
| GMS | *1.00 | 0.84 | 1.08 | 1.09 | 1.10 | 1.06 |
| GMS | *1.05 | 0.85 | 1.09 | 1.09 | 1.11 | 1.07 |
| GMS | *1.15 | 0.87 | 1.09 | 1.10 | 1.12 | 1.08 |
| GMS | *1.25 | 0.88 | 1.10 | 1.10 | 1.13 | 1.09 |
| GMS | 250 m | 1.10 | 1.17 | 1.12 | 1.20 | 1.16 |
| GMS | 500 m | 0.87 | 1.09 | 1.09 | 1.11 | 1.08 |
| GMS | 1000 m | 0.65 | 1.00 | 1.05 | 1.02 | 0.98 |
| NSS | *0.75 | 1.43 | 1.32 | 1.13 | 1.31 | 1.30 |
| NSS | *0.85 | 1.43 | 1.32 | 1.13 | 1.34 | 1.30 |
| NSS | *0.95 | 1.44 | 1.32 | 1.13 | 1.36 | 1.30 |
| NSS | *1.00 | 1.55 | 1.32 | 1.13 | 1.37 | 1.30 |
| NSS | *1.05 | 1.52 | 1.32 | 1.13 | 1.37 | 1.30 |
| NSS | *1.15 | 1.41 | 1.33 | 1.13 | 1.39 | 1.31 |
| NSS | *1.25 | 2.16 | 1.34 | 1.13 | 1.40 | 1.31 |
| NSS | 500 m | 1.06 | 1.23 | 1.11 | 1.22 | 1.21 |
| NSS | 1000 m | 0.79 | 1.12 | 1.08 | 1.09 | 1.11 |
| NSC | *0.75 | 1.04 | 1.24 | 1.09 | 1.18 | 1.25 |
| NSC | *0.85 | 1.06 | 1.24 | 1.10 | 1.20 | 1.25 |
| NSC | *0.95 | 1.13 | 1.25 | 1.09 | 1.22 | 1.26 |
| NSC | *1.00 | 1.12 | 1.26 | 1.10 | 1.24 | 1.27 |
| NSC | 500 m | 1.00 | 1.20 | 1.09 | 1.17 | 1.22 |
| NSC | 1000 m | 0.64 | 1.08 | 1.05 | 1.04 | 1.10 |
| AVG. | | 1.14 | 1.21 | 1.10 | 1.22 | 1.20 |
| C.O.V | | 0.32 | 0.09 | 0.02 | 0.10 | 0.09 |

**Table 15**

Initial Load and Capacity Factors
for Minimum Tension (beta=3.5)

| TLP | Case | Tsd | Tm | T1v | T2v | Tw-sp |
|---|---|---|---|---|---|---|
| GMS | *1.00 | 1.02 | 1.33 | 1.22 | 1.45 | 1.30 |
| GMS | *1.05 | 1.04 | 1.34 | 1.22 | 1.47 | 1.31 |
| GMS | *1.15 | 1.06 | 1.34 | 1.22 | 1.49 | 1.32 |
| GMS | *1.25 | 1.10 | 1.35 | 1.23 | 1.51 | 1.33 |
| GMS | 250 m | 1.43 | 1.45 | 1.26 | 1.58 | 1.42 |
| GMS | 500 m | 1.05 | 1.34 | 1.22 | 1.46 | 1.32 |
| GMS | 1000 m | 0.76 | 1.23 | 1.17 | 1.35 | 1.21 |
| NSS | *0.75 | 2.20 | 1.71 | 1.28 | 1.72 | 1.68 |
| NSS | *0.85 | 2.15 | 1.70 | 1.27 | 1.81 | 1.67 |
| NSS | *0.95 | 2.18 | 1.71 | 1.28 | 1.89 | 1.68 |
| NSS | *1.00 | 2.35 | 1.71 | 1.28 | 1.91 | 1.68 |
| NSS | *1.05 | 2.40 | 1.72 | 1.27 | 1.93 | 1.69 |
| NSS | *1.15 | 1.83 | 1.71 | 1.28 | 1.97 | 1.69 |
| NSS | *1.25 | 2.73 | 1.73 | 1.27 | 2.01 | 1.70 |
| NSS | 500 m | 1.37 | 1.55 | 1.24 | 1.62 | 1.52 |
| NSS | 1000 m | 0.96 | 1.41 | 1.21 | 1.43 | 1.39 |
| NSC | *0.75 | 1.32 | 1.60 | 1.22 | 1.45 | 1.60 |
| NSC | *0.85 | 1.39 | 1.59 | 1.22 | 1.54 | 1.60 |
| NSC | *0.95 | 1.52 | 1.60 | 1.23 | 1.61 | 1.61 |
| NSC | *1.00 | 1.47 | 1.60 | 1.23 | 1.65 | 1.61 |
| NSC | 500 m | 1.26 | 1.53 | 1.21 | 1.55 | 1.54 |
| NSC | 1000 m | 0.78 | 1.38 | 1.16 | 1.36 | 1.39 |
| AVG. | | 1.54 | 1.54 | 1.24 | 1.63 | 1.52 |
| C.O.V | | 0.38 | 0.11 | 0.03 | 0.13 | 0.11 |

**Table 16**
Load and Capacity Factors
for Minimum Tension (beta=3)

| Factor | Initial | Optimized |
|---|---|---|
| Tsd | 1.14 | 0.87 |
| Tmom | 1.21 | 1.30 |
| Tdyn | 1.00 | 1.00 |
| T1v | 1.10 | 1.10 |
| T2v | 1.22 | 1.22 |
| Tw-sp | 1.20 | 1.20 |
| residual mean square | 0.17 | 0.04 |

**Table 17**
Load and Capacity Factors
for Minimum Tension (beta=3.5)

| Factor | Initial | Optimized |
|---|---|---|
| Tsd | 1.54 | 1.00 |
| Tmom | 1.54 | 1.65 |
| Tdyn | 1.00 | 1.00 |
| T1v | 1.24 | 1.24 |
| T2v | 1.63 | 1.63 |
| Tw-sp | 1.52 | 1.52 |
| residual mean squared | 0.30 | 0.07 |

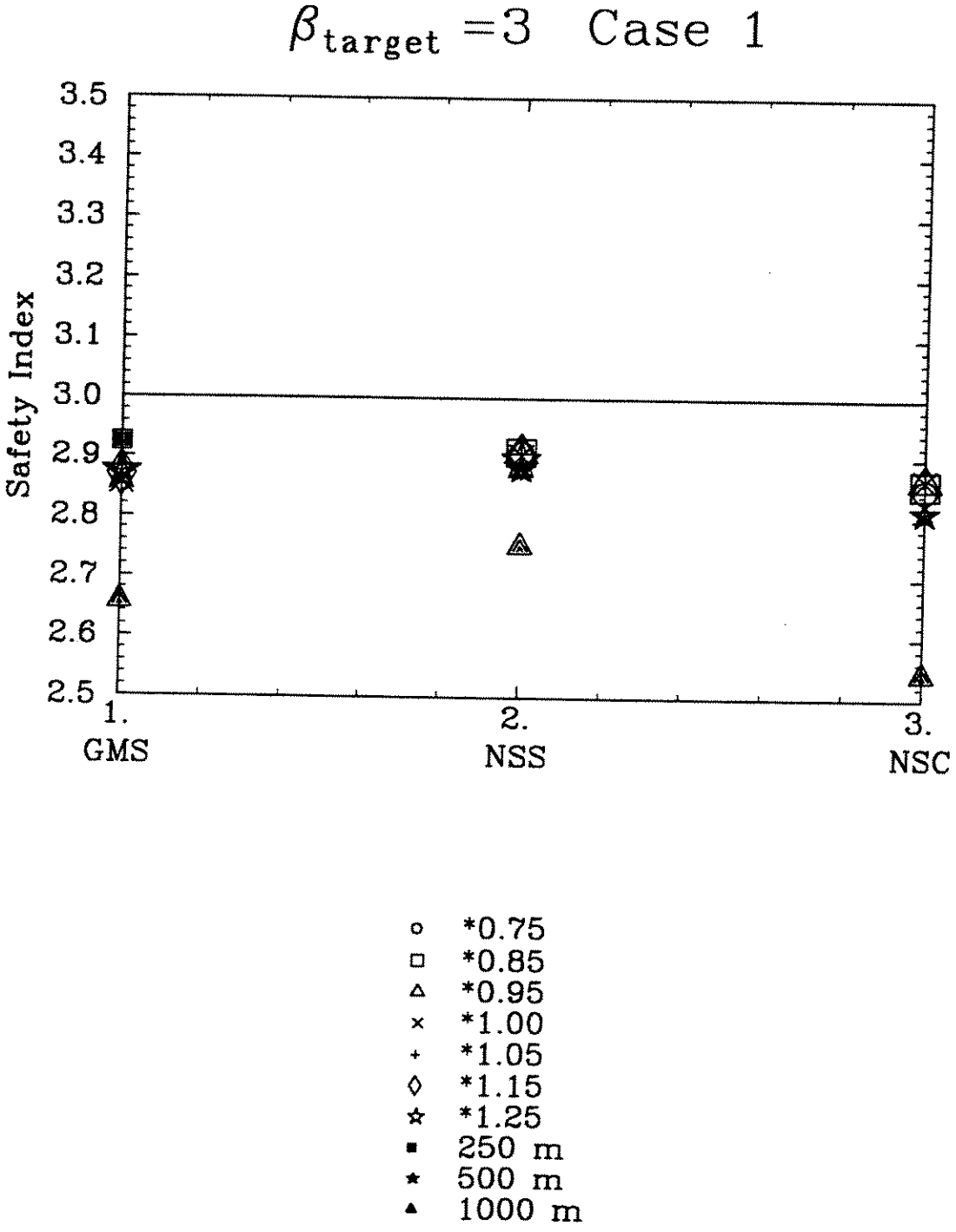


**Figure 13.** Safety indices for minimum tension obtained using the initial load factors; target safety index: 3.

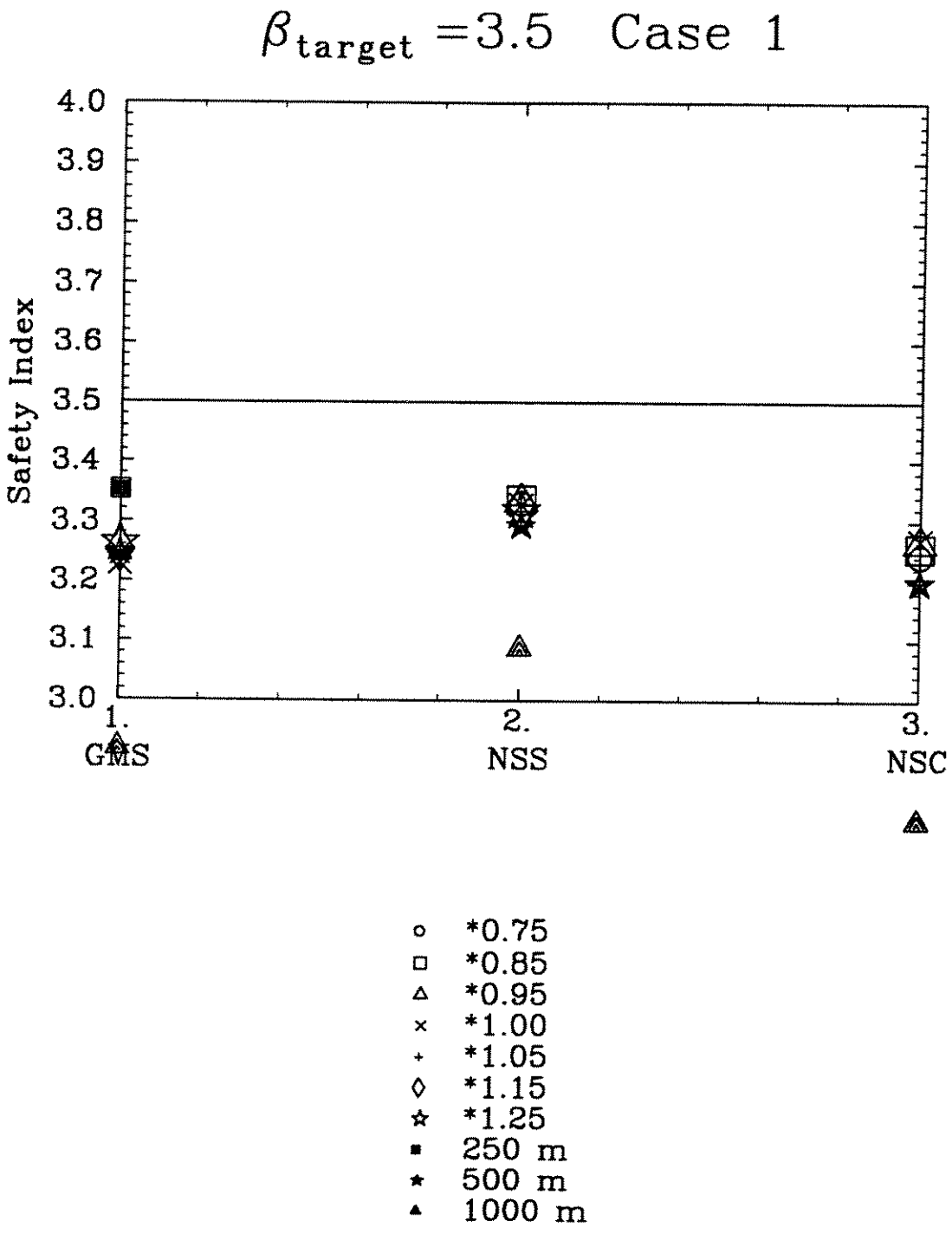


**Figure 14.** Safety indices for minimum tension obtained using the initial load factors; target safety index: 3.5.

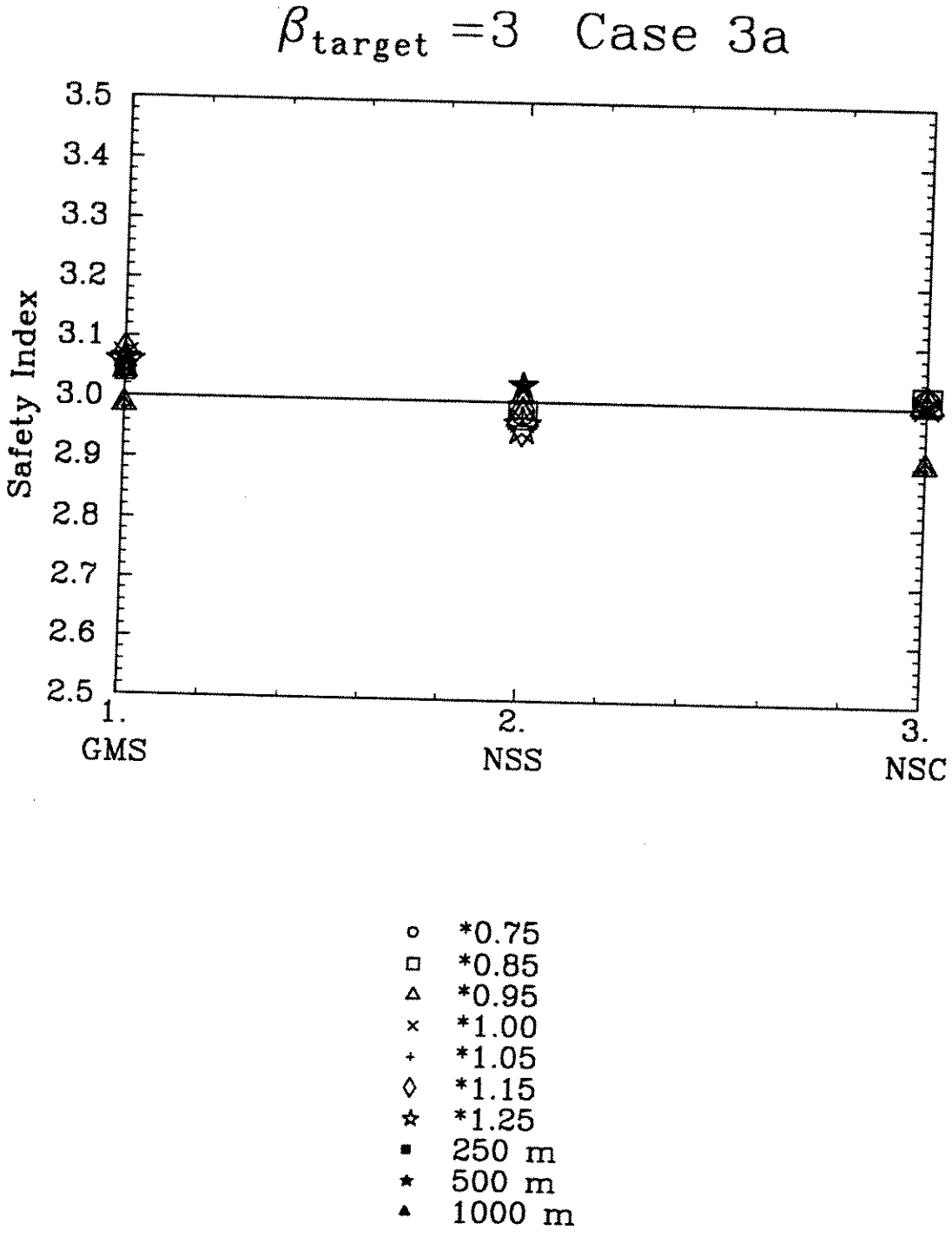


**Figure 15.** Safety indices for minimum tension obtained using the optimized load factors; target safety index: 3.

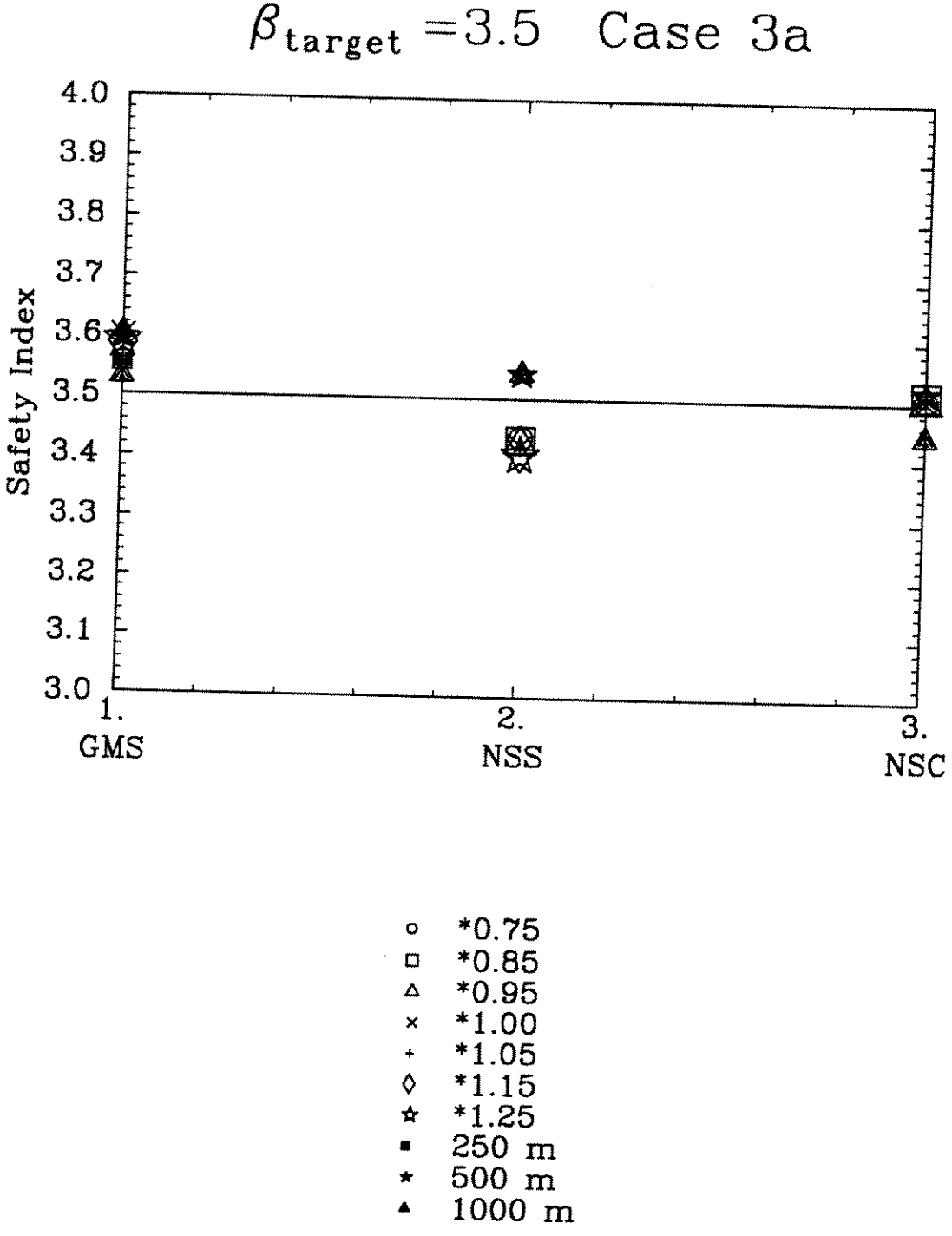


**Figure 16.** Safety indices for minimum tension obtained using the optimized load factors; target safety index: 3.5.

## CALIBRATION FOR AIR GAP

Air gap is treated as a safety related limit state because wave impact on the deck generates large tensions on the tendons. Commonly, these tensions are not considering when sizing the tendons, relying instead on a large enough air gap so that wave impact is unlikely. The calibration process for air gap is similar to that followed for maximum offset and minimum tension. The checking equation for air gap is of the form

$$G_{min} = \gamma_\eta \eta + \gamma_{su} Z_{su} + \gamma_{td} Z_{td} + \gamma_{sd} \left[ L - \sqrt{L^2 - X_{max}^2} \right] \quad (10)$$

where G stands for air gap, $\eta$ is the characteristic wave crest elevation (modified by the wave-enhancement factor), $Z_{su}$ and $Z_{td}$ are the characteristic values of storm surge and astronomical tide, and $X_{max}$ is the maximum offset calculated using Equation 8 and the load factors for offset obtained in the calibration of maximum offset (Tables 11 and 13).

Calibration is performed for safety indices of 3 and 4. For the safety index of 4, two calibrations are performed, using the 100 and 1000-year characteristic environments. Tables 18 through 20 show the calculation of the initial load factors for air gap. The load factors show little variability across platforms. Figures 17 and 18 show the safety indices associated with the initial load factors for the 100-year characteristic environments. These figures show, on average, a tendency to overpredict the required air gap. These figures also show a significant differences among the safety indices of the three platforms. Figure 19 shows the initial load factors for the safety index of 4 and the 1000-year characteristic environment. This figure shows a tendency to over-predict air gap and differences among platforms, but to much lesser extent than figure 18.

Tables 18 through 20 also show that the initial load factors for tide are very low (i.e., near 0.1). This is because the effect of tide on air gap is partially offset by increased pretension, which tends to reduce lateral offset. In addition, we used a uniform distribution for tide, whereas the true distribution of tide has more mass near its lower and upper bounds than a uniform distribution [18]. The effect of tide would have been somewhat larger if we had used the correct distribution.

The optimal adjustment to the load factors consisted on setting the factor for setdown ($\gamma_{sd}$) to

[18] A better approximation to the true distribution of tide is the distribution of $\cos(\theta)$, where $\theta$ is uniformly distributed between 0 and 180 degrees. This distribution has a larger mass near 1 than near 0 because the cosine function spends more "time" near its lower and upper bounds than near 0.

0.85, for all cases considered (see Tables 21 through 23)[19]. In addition, the coefficient for tide ($\gamma_{td}$) is set to 1.00, at the cost of increased mean-square error, because values near 0.10 would look counter-intuitive to the designer. The safety indices corresponding to these adjusted load factors are shown in Figures 20 through 22. These figures indicate that the variability across platforms is still present, especially for the calibrations than use the 100-year characteristic environment. The overall scatter in safety indices is moderate, indicating that the load factors for air gap result in reasonable estimates of maximum offset. As expected, the use of the 1000-year characteristic environment leads to more consistent estimates of the air gap associated with a safety index of 4 than using the 100-year characteristic environment.

[19]We have not calculated the offset load factors in Equation 8 for the safety index of 4 and the 1000-year characteristic environment. Thus, we use the initial estimates of these factors from Table 20 (with slight changes), and we include these values in Table 23.

**Table 18**
Initial Part. Load and Capacity Factors for Air Gap (beta=3)

| TLP | Case | Xs | X1v | Xlfw | X2v | Crest | Surge | Tide |
|---|---|---|---|---|---|---|---|---|
| GMS | *1.00 | 1.55 | 1.23 | 1.62 | 1.14 | 1.19 | 1.17 | 0.10 |
| GMS | *1.05 | 1.55 | 1.23 | 1.61 | 1.16 | 1.19 | 1.17 | 0.11 |
| GMS | *1.15 | 1.56 | 1.25 | 1.60 | 1.17 | 1.19 | 1.17 | 0.11 |
| GMS | *1.25 | 1.56 | 1.26 | 1.58 | 1.19 | 1.19 | 1.17 | 0.12 |
| GMS | 250 m | 1.54 | 1.25 | 1.44 | 1.14 | 1.20 | 1.18 | 0.13 |
| GMS | 500 m | 1.55 | 1.23 | 1.43 | 1.14 | 1.19 | 1.17 | 0.11 |
| GMS | 1000 m | 1.53 | 1.21 | 1.40 | 1.14 | 1.17 | 1.15 | 0.08 |
| NSS | *0.75 | 1.53 | 1.26 | 0.96 | 1.09 | 1.20 | 1.18 | 0.15 |
| NSS | *0.85 | 1.52 | 1.27 | 1.05 | 1.14 | 1.20 | 1.18 | 0.16 |
| NSS | *0.95 | 1.51 | 1.30 | 1.13 | 1.16 | 1.20 | 1.18 | 0.17 |
| NSS | *1.00 | 1.52 | 1.30 | 1.15 | 1.17 | 1.20 | 1.18 | 0.17 |
| NSS | *1.05 | 1.50 | 1.32 | 1.18 | 1.18 | 1.20 | 1.19 | 0.18 |
| NSS | *1.15 | 1.50 | 1.34 | 1.22 | 1.20 | 1.20 | 1.19 | 0.19 |
| NSS | *1.25 | 1.49 | 1.37 | 1.25 | 1.21 | 1.21 | 1.19 | 0.19 |
| NSS | 500 m | 1.57 | 1.28 | 1.48 | 1.17 | 1.19 | 1.17 | 0.12 |
| NSS | 1000 m | 1.55 | 1.25 | 1.45 | 1.16 | 1.16 | 1.15 | 0.08 |
| NSC | *0.75 | 1.58 | 1.27 | 1.70 | 1.04 | 1.19 | 1.17 | 0.09 |
| NSC | *0.85 | 1.59 | 1.31 | 1.73 | 1.11 | 1.19 | 1.18 | 0.10 |
| NSC | *0.95 | 1.60 | 1.33 | 1.74 | 1.15 | 1.20 | 1.18 | 0.11 |
| NSC | *1.00 | 1.60 | 1.35 | 1.73 | 1.16 | 1.20 | 1.18 | 0.11 |
| NSC | 500 m | 1.58 | 1.33 | 1.60 | 1.15 | 1.19 | 1.17 | 0.11 |
| NSC | 1000 m | 1.55 | 1.29 | 1.56 | 1.14 | 1.16 | 1.15 | 0.07 |
| AVG. | | 1.55 | 1.29 | 1.43 | 1.15 | 1.19 | 1.17 | 0.13 |
| C.O.V | | 0.02 | 0.03 | 0.17 | 0.03 | 0.01 | 0.01 | 0.30 |

**Table 19**
Initial Load and Capacity Factors for Air Gap
(beta=4, characteristic environment: 100 yrs)

| TLP | Case | Xs | X1v | Xlfw | X2v | Crest | Surge | Tide |
|---|---|---|---|---|---|---|---|---|
| GMS | *1.00 | 2.30 | 1.55 | 2.61 | 1.27 | 1.42 | 1.40 | 0.06 |
| GMS | *1.05 | 2.31 | 1.56 | 2.60 | 1.32 | 1.42 | 1.40 | 0.06 |
| GMS | *1.15 | 2.34 | 1.59 | 2.59 | 1.37 | 1.43 | 1.40 | 0.07 |
| GMS | *.125 | 2.35 | 1.61 | 2.56 | 1.42 | 1.43 | 1.40 | 0.08 |
| GMS | 250 m | 2.32 | 1.58 | 2.22 | 1.27 | 1.44 | 1.41 | 0.10 |
| GMS | 500 m | 2.29 | 1.55 | 2.18 | 1.28 | 1.42 | 1.40 | 0.07 |
| GMS | 1000 m | 2.21 | 1.51 | 2.09 | 1.28 | 1.39 | 1.38 | 0.04 |
| NSS | *0.75 | 2.29 | 1.62 | 1.08 | 1.12 | 1.45 | 1.42 | 0.12 |
| NSS | *0.85 | 2.31 | 1.65 | 1.25 | 1.24 | 1.45 | 1.42 | 0.13 |
| NSS | *0.95 | 2.30 | 1.69 | 1.39 | 1.33 | 1.45 | 1.42 | 0.15 |
| NSS | *1.00 | 2.30 | 1.71 | 1.46 | 1.35 | 1.45 | 1.42 | 0.16 |
| NSS | *1.05 | 2.30 | 1.75 | 1.52 | 1.39 | 1.46 | 1.42 | 0.16 |
| NSS | *1.15 | 2.30 | 1.80 | 1.62 | 1.42 | 1.46 | 1.42 | 0.17 |
| NSS | *1.25 | 2.28 | 1.87 | 1.69 | 1.47 | 1.46 | 1.42 | 0.18 |
| NSS | 500 m | 2.40 | 1.66 | 2.45 | 1.36 | 1.42 | 1.40 | 0.07 |
| NSS | 1000 m | 2.30 | 1.61 | 2.30 | 1.35 | 1.38 | 1.37 | 0.04 |
| NSC | *0.75 | 2.28 | 1.59 | 2.51 | 0.99 | 1.39 | 1.37 | 0.02 |
| NSC | *0.85 | 2.31 | 1.64 | 2.70 | 1.15 | 1.38 | 1.37 | 0.03 |
| NSC | *0.95 | 2.33 | 1.70 | 2.85 | 1.25 | 1.38 | 1.37 | 0.03 |
| NSC | *1.00 | 2.34 | 1.73 | 2.89 | 1.28 | 1.38 | 1.37 | 0.04 |
| NSC | 500 m | 2.30 | 1.72 | 2.93 | 1.28 | 1.38 | 1.36 | 0.04 |
| NSC | 1000 m | 2.18 | 1.68 | 2.72 | 1.28 | 1.36 | 1.35 | 0.03 |
| AVG. | | 2.30 | 1.66 | 2.17 | 1.29 | 1.42 | 1.39 | 0.09 |
| C.O.V | | 0.02 | 0.05 | 0.27 | 0.08 | 0.02 | 0.02 | 0.63 |

**Table 20**
Initial Load and Capacity Factors for Air Gap
(beta=4, characteristic environment: 1000 yrs)

| TLP | Case | Xs | X1v | Xlfw | X2v | Crest | Surge | Tide |
|---|---|---|---|---|---|---|---|---|
| GMS | *1.00 | 1.68 | 1.18 | 2.00 | 1.10 | 1.15 | 1.14 | 0.06 |
| GMS | *1.05 | 1.68 | 1.18 | 1.97 | 1.12 | 1.15 | 1.14 | 0.06 |
| GMS | *1.15 | 1.69 | 1.19 | 1.93 | 1.14 | 1.16 | 1.14 | 0.07 |
| GMS | *.125 | 1.70 | 1.20 | 1.89 | 1.16 | 1.16 | 1.14 | 0.08 |
| GMS | 250 m | 1.64 | 1.20 | 1.54 | 1.10 | 1.17 | 1.15 | 0.10 |
| GMS | 500 m | 1.67 | 1.18 | 1.53 | 1.10 | 1.15 | 1.14 | 0.07 |
| GMS | 1000 m | 1.66 | 1.15 | 1.49 | 1.10 | 1.13 | 1.12 | 0.04 |
| NSS | *0.75 | 1.60 | 1.21 | 0.80 | 1.01 | 1.17 | 1.15 | 0.12 |
| NSS | *0.85 | 1.61 | 1.23 | 0.92 | 1.06 | 1.18 | 1.15 | 0.13 |
| NSS | *0.95 | 1.60 | 1.23 | 1.01 | 1.11 | 1.18 | 1.15 | 0.15 |
| NSS | *1.00 | 1.59 | 1.24 | 1.05 | 1.12 | 1.18 | 1.16 | 0.16 |
| NSS | *1.05 | 1.58 | 1.25 | 1.09 | 1.13 | 1.18 | 1.16 | 0.16 |
| NSS | *1.15 | 1.59 | 1.27 | 1.16 | 1.14 | 1.18 | 1.16 | 0.17 |
| NSS | *1.25 | 1.56 | 1.28 | 1.20 | 1.16 | 1.18 | 1.16 | 0.18 |
| NSS | 500 m | 1.72 | 1.21 | 1.73 | 1.12 | 1.15 | 1.14 | 0.07 |
| NSS | 1000 m | 1.70 | 1.17 | 1.65 | 1.11 | 1.12 | 1.11 | 0.04 |
| NSC | *0.75 | 1.66 | 1.16 | 2.01 | 0.97 | 1.12 | 1.11 | 0.02 |
| NSC | *0.85 | 1.66 | 1.17 | 2.13 | 1.04 | 1.12 | 1.11 | 0.03 |
| NSC | *0.95 | 1.67 | 1.18 | 2.21 | 1.07 | 1.12 | 1.11 | 0.03 |
| NSC | *1.00 | 1.67 | 1.19 | 2.23 | 1.08 | 1.12 | 1.11 | 0.04 |
| NSC | 500 m | 1.66 | 1.19 | 2.06 | 1.09 | 1.12 | 1.11 | 0.04 |
| NSC | 1000 m | 1.63 | 1.16 | 1.94 | 1.08 | 1.10 | 1.09 | 0.03 |
| AVG. | | 1.64 | 1.20 | 1.60 | 1.10 | 1.15 | 1.13 | 0.09 |
| C.O.V | | 0.03 | 0.03 | 0.29 | 0.04 | 0.02 | 0.02 | 0.63 |

**Table 21**
Load and Capacity Factors
for Air Gap (beta=3)

| Factor | Initial | Optimized |
|---|---|---|
| Crest | 1.19 | 1.20 |
| Surge | 1.17 | 1.17 |
| Tide | 0.13 | 1.00 |
| Setdown | 1.00 | 0.85 |
| residual mean square | 0.10 | 0.10 |

**Table 22**
Load and Capacity Factors
for Air Gap (beta=4,
characteristic environment=100 yrs)

| Factor | Initial | Optimized |
|---|---|---|
| Crest | 1.42 | 1.40 |
| Surge | 1.39 | 1.39 |
| Tide | 0.13 | 1.00 |
| Setdown | 1.00 | 0.85 |
| residual mean square | 0.25 | 0.17 |

**Table 23**
Load and Capacity Factors
for Air Gap (beta=4,
characteristic environment=1000 yrs)

| Factor | Initial | Optimized |
|---|---|---|
| Crest | 1.15 | 1.15 |
| Surge | 1.13 | 1.13 |
| Tide | 0.09 | 1.00 |
| Setdown | 1.00 | 0.85 |
| Xs | 1.64 | 1.6 |
| Xdyn | 1.00 | 1.00 |
| X1v | 1.20 | 1.20 |
| Xlfw | 1.60 | 1.60 |
| X2v | 1.10 | 1.10 |
| residual mean square | 0.13 | 0.07 |

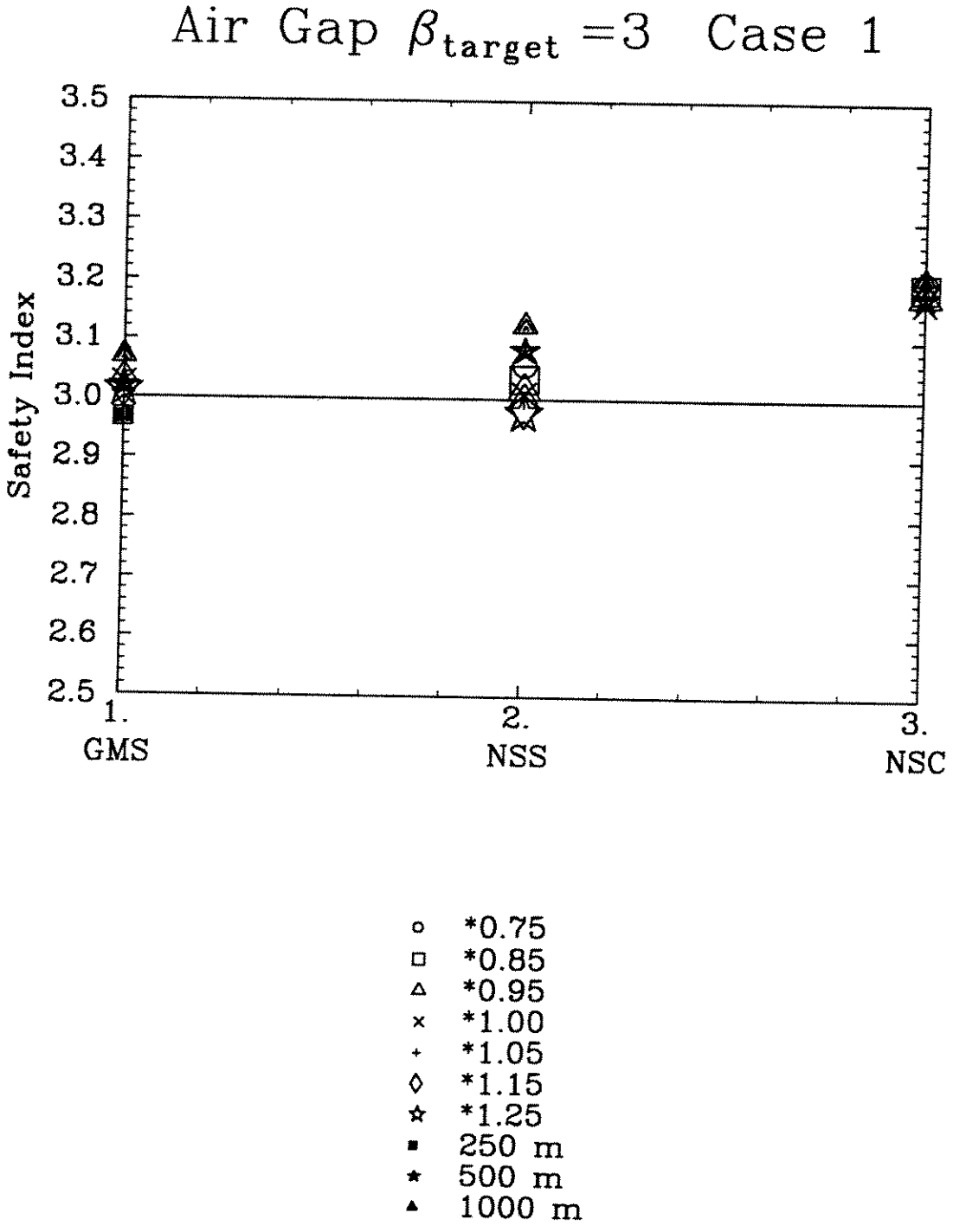


**Figure 17.** Safety indices for air gap obtained using the load factors; target safety index: 3..

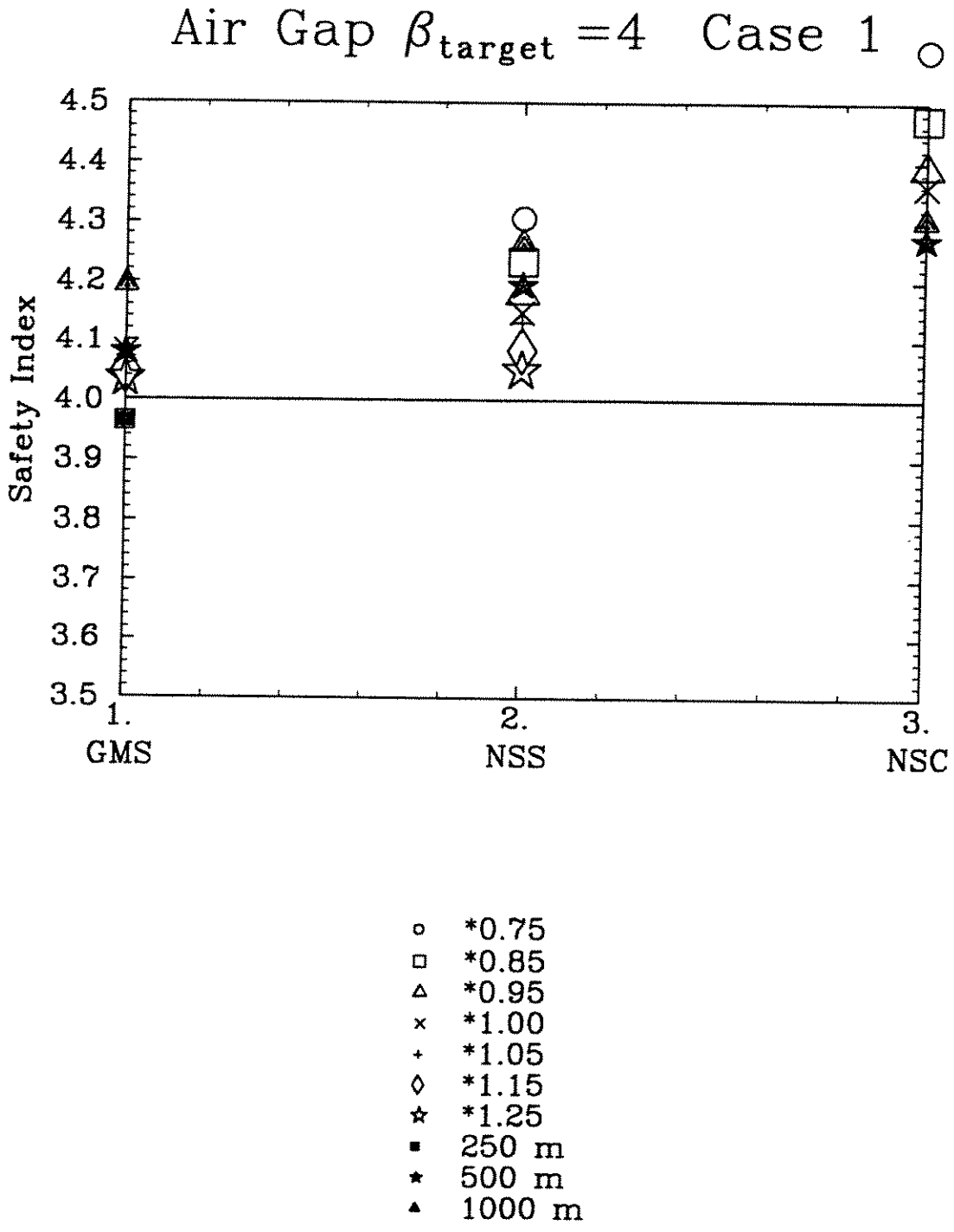


**Figure 18.** Safety indices for air gap obtained using the initial load factors; target safety index: 4; characteristic environment: 100 years.

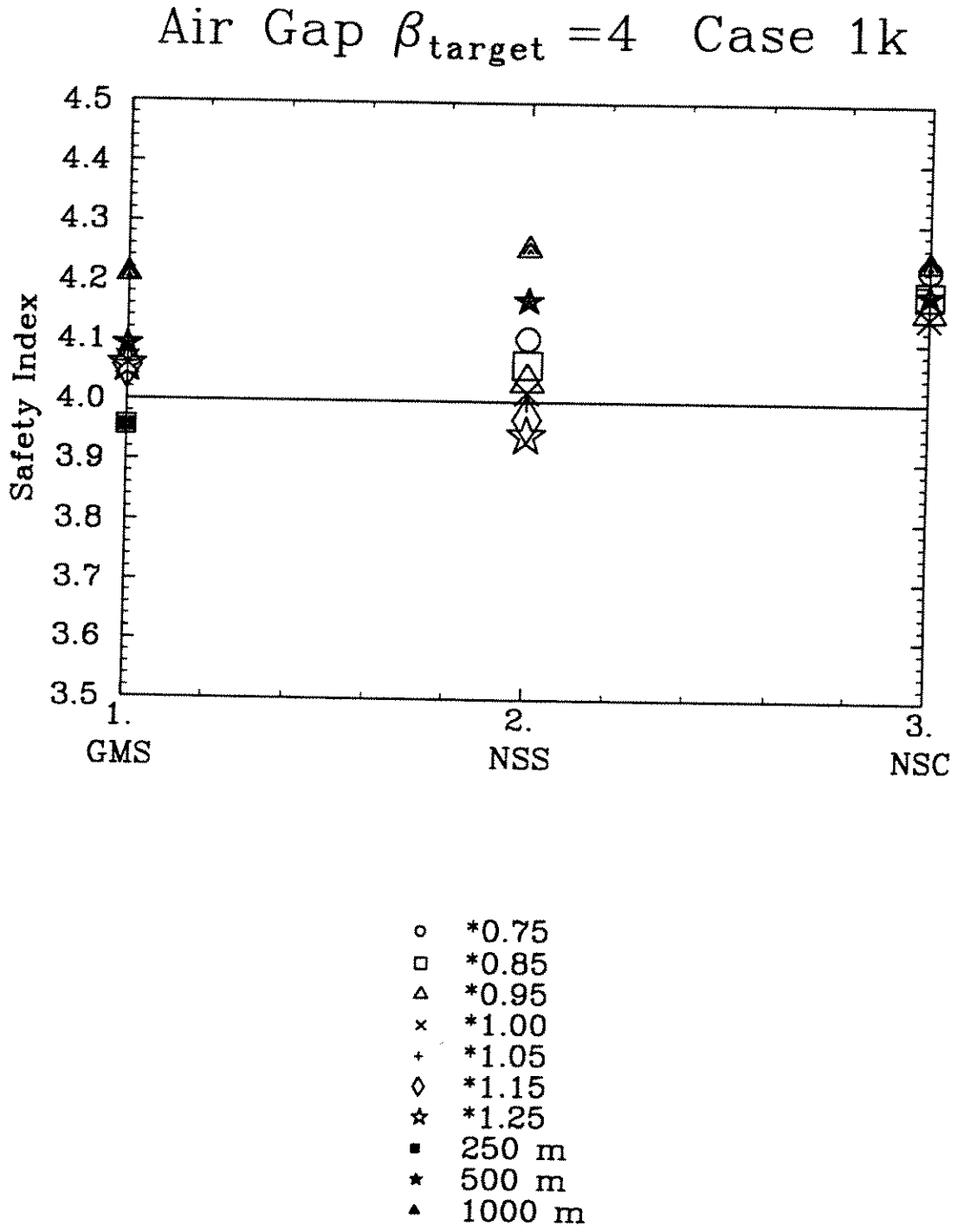


**Figure 19.** Safety indices for air gap obtained using the initial load factors; target safety index: 4; characteristic environment: 1000 years.

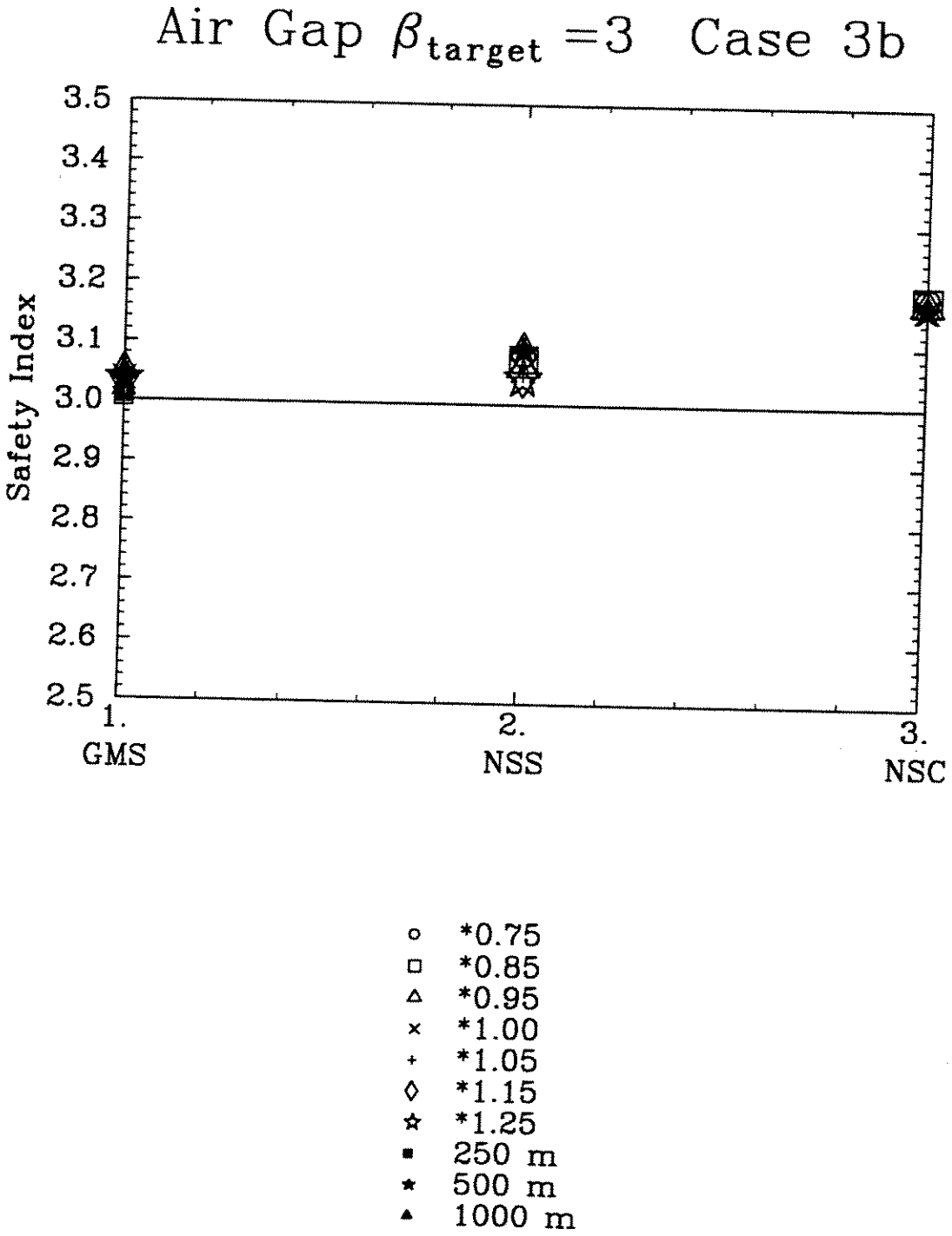


**Figure 20.** Safety indices for air gap obtained using the optimized load factors; target safety index: 3.

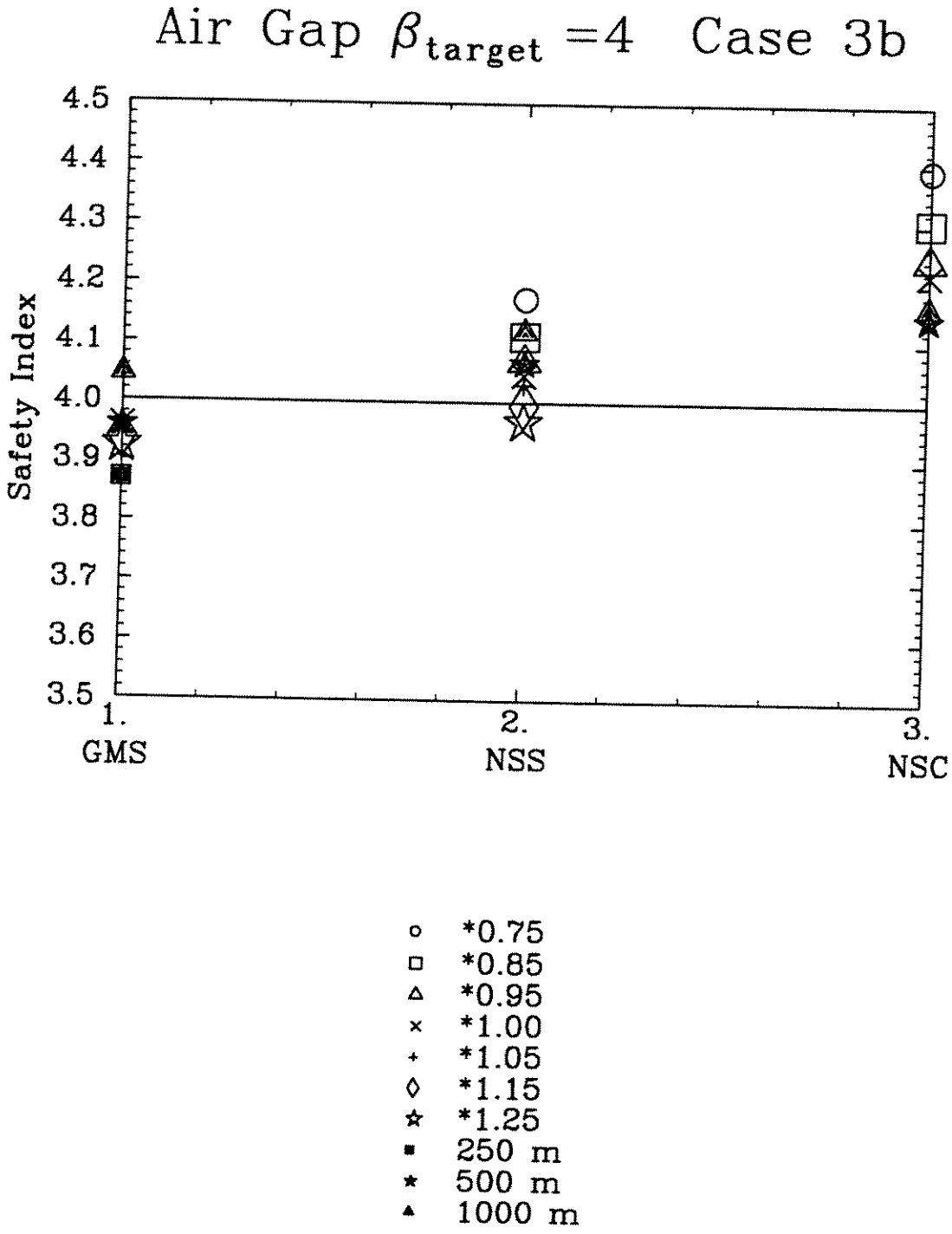


**Figure 21.** Safety indices for air gap obtained using the optimized load factors; target safety index: 4; characteristic environment: 100 years.

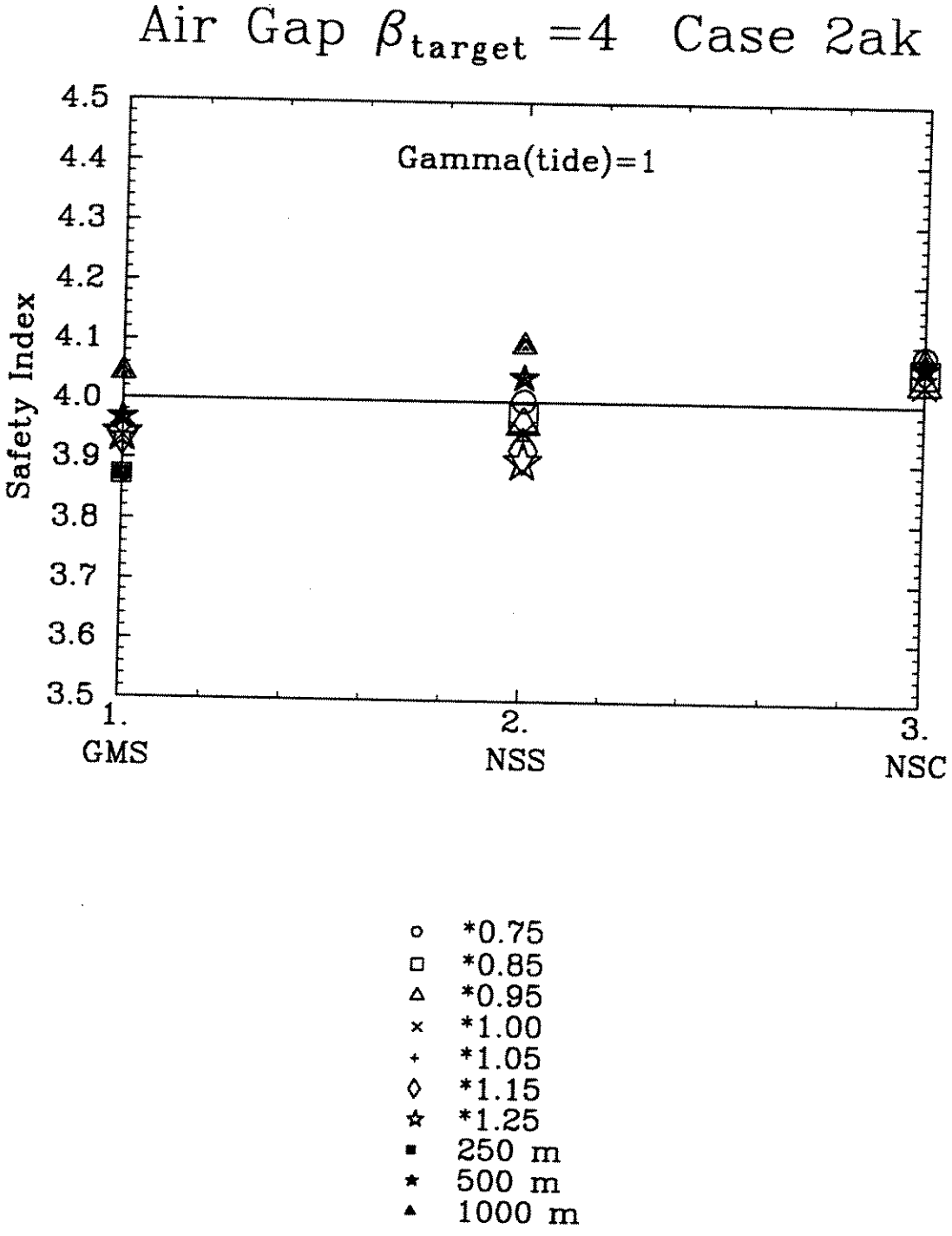


**Figure 22.** Safety indices for air gap obtained using the optimized load factors; target safety index: 4; characteristic environment: 1000 years.

## SUMMARY AND DISCUSSION

This study has demonstrated the feasibility of reliability based calibration of design equations for TLP global responses, using separate factors for the various components of static and dynamic response. The calculated load and capacity factors for tendon capacity lead to designs with safety indices near the target safety index. Similarly, the calculated load factors for maximum offset, minimum tension, and air gap, lead to accurate predictions of the global response associated with a certain exceedance probability. For all limit states except air gap, use of a 100-year characteristic environment and appropriate factors proved adequate for safety indices of up to 3.5 or 4. For air gap and a safety index of 4, the 1000-year characteristic environment is preferable. The significant differences among the load factors obtained for the various static and dynamic response components underscore the need for multiple load factors.

The three existing and 19 scaled platforms considered in this calibration cover a range of water depths from 150 to 1000 m, and a range of sizes extending from platforms as small as Jolliett to platforms as large as Heidrun. Future calibration efforts should consider additional designs based on actual platforms and should include a re-assessment of the response equations for scaled platforms.

The load and capacity factors obtained here are robust with respect to moderate changes in the parameters and assumptions used in the reliability calculations, but not to major changes. For instance, modification of the order of 20% to the bias for first-order tension (to account for the non-Gaussian character of the response) would not require changes in the load factors. Similarly, moderate increases in the subjective uncertainties would not require changes in the load factors. On the other hand, the load and capacity factors obtained here for a Gulf of Mexico environment would likely not be applicable to North Sea environments.

## REFERENCES

Offshore Systems Analysis Corporation, OSAC (1992). TLP Regression Analysies for Gulf of Mexico Environments. Report to Conoco, Inc., November.

Risk Engineering, Inc. (1992). Model Code for Design of Floating Platforms—Phase I: Probabilistic Modeling, December.

Thoft-Christiansen, P., and M. Baker (1982). *Structural Reliability Theory and its Applications*. Springer Verlag, Berlin.